DESIGN AND CONSTRUCTION OF AN IODINE LASER OSCILLATOR

Frederick Charles Marcell

NAVAL POSTGRADUATE SCHOOL
Monterey, California

THESIS

DESIGN AND CONSTRUCTION OF
AN IODINE LASER OSCILLATOR

by

Frederick Charles Marcell Jr.

June 1976

Thesis Advisor: F. R. Schwirzke

Unclassified

SECURITY CLASSIFICATION OF THIS PAGE (When Data Entered)

REPORT DOCUMENTATION PAGE		READ INSTRUCTIONS BEFORE COMPLETING FORM
1. REPORT NUMBER	2. GOVT ACCESSION NO.	3. RECIPIENT'S CATALOG NUMBER
4. TITLE (and Subtitle) Design and Construction of an Iodine Laser Oscillator		5. TYPE OF REPORT & PERIOD COVERED Master's Thesis; June 1976 6. PERFORMING ORG. REPORT NUMBER
7. AUTHOR(s) Frederick Charles Marcell Jr.		8. CONTRACT OR GRANT NUMBER(s)
9. PERFORMING ORGANIZATION NAME AND ADDRESS Naval Postgraduate School Monterey, California 93940		10. PROGRAM ELEMENT, PROJECT, TASK AREA & WORK UNIT NUMBERS
11. CONTROLLING OFFICE NAME AND ADDRESS Naval Postgraduate School Monterey, California 93940		12. REPORT DATE June 1976 13. NUMBER OF PAGES
14. MONITORING AGENCY NAME & ADDRESS(if different from Controlling Office) Naval Postgraduate School Monterey, California 93940		15. SECURITY CLASS. (of this report) Unclassified 15a. DECLASSIFICATION/DOWNGRADING SCHEDULE

16. DISTRIBUTION STATEMENT (of this Report)

Approved for public release; distribution unlimited.

17. DISTRIBUTION STATEMENT (of the abstract entered in Block 20, if different from Report)

18. SUPPLEMENTARY NOTES

19. KEY WORDS (Continue on reverse side if necessary and identify by block number)

Photodissociation laser
Gas laser
Iodine laser
Chemical laser

20. ABSTRACT (Continue on reverse side if necessary and identify by block number)

A small photochemical dissociation gas laser oscillator has been constructed for use in the study of laser characteristics, energy extraction techniques, and plasma production. It operates with a mixture of perfluorinated-propyliodide and argon as an active medium. The laser is pumped by ultraviolet light in a 500 A wide band centered around 2680 A. The light is produced by passing a large electric current through two

DD FORM 1 JAN 73 1473 EDITION OF 1 NOV 65 IS OBSOLETE
S/N 0102-014-6601 |
(Page 1)

Unclassified
SECURITY CLASSIFICATION OF THIS PAGE (When Data Entered)

parallel-mounted xenon-filled flashtubes, and causes excitation of the C_3F_7I molecule which dissociates to a radical $[C_3F_7]$ and iodine $[I^*]$ in the state $I(^2P_{1/2})$. The resulting forbidden magnetic dipole transition $I(^2P_{1/2}) \rightarrow I(^2P_{3/2})$ produces laser action at wavelength $\lambda = 1.315$ μm. The laser uses a hemo-confocal optical cavity. It consists of a spherical mirror with a radius of 1.5 m and reflectance of ∿ 98% and a planar mirror with a reflectance of ∿ 75% separated by ∿ 86 cm. Design considerations predict a pulsed output in the range of 1-10 millijoules in a pulse length of 2-10 nsec for a pumping energy of ∿ 300 to 400 joules.

Design and Construction of an Iodine Laser Oscillator

by

Frederick Charles Marcell Jr.
Lieutenant, United States Navy
BSEE, University of Colorado, 1970

Submitted in partial fulfillment of the
requirements for the degree of

MASTER OF SCIENCE IN PHYSICS

from the

NAVAL POSTGRADUATE SCHOOL

June 1976

ABSTRACT

A small photochemical dissociation gas laser oscillator has been constructed for use in the study of laser characteristics, energy extraction techniques, and plasma production. It operates with a mixture of perfluorinated-propyliodide and argon as an active medium. The laser is pumped by ultraviolet light in a 500Å wide band centered around 2680Å. The light is produced by passing a large electric current through two parallel-mounted xenon-filled flashtubes, and causes excitation of the C_3F_7I molecule which dissociates to a radical $[C_3F_7]$ and iodine [I*] in the state $I(^2P_{\frac{1}{2}})$. The resulting forbidden magnetic dipole transition $I(^2P_{\frac{1}{2}}) \rightarrow I(^2P_{\frac{3}{2}})$ produces laser action at wavelength $\lambda = 1.315$ μm. The laser uses a hemiconfocal optical cavity. It consists of a spherical mirror with a radius of 1.5 m and reflectance of ∿ 98% and a planar mirror with a reflectance of ∿ 75% separated by ∿ 86 cm. Design considerations predict a pulsed output in the range of 1-10 millijoules in a pulse length of ∿ 2-10 nsec for a pumping energy of ∿ 300 to 400 joules.

TABLE OF CONTENTS

LIST OF ILLUSTRATIONS
(COLLECTED IN APPENDIX D)

ACKNOWLEDGEMENTS

Numerous people have contributed ideas, time, effort, and equipment to this project. I express heartfelt gratitude to all of them. Special thanks are in order for Mr. Robert Sanders for his many hours of expert technical assistance, trying to make the laser and the test equipment work; to Mr. Peter Whistler and his fine staff of machinists at NPS machine facility who not only contributed to design, but turned ideas into reality; to Messrs. Ted Dutton and Robert Moeller who devoted time listening to my schemes and donating components; to Mr. Tom Maris for coating my mirrors; to Professor Ed Dally, who not only donated equipment and ideas, but time to trouble-shoot the high voltage trigger system; to Professors Crittenden and Tolles for the time they took to discuss concepts in the early stages of design; to Mr. Hal Herreman for his help in the laboratory even after his retirement, and to my lab mates, Syd Shewchuck, John Jacobson, Francis Williamson, and Dan Callahan who all showed so much interest in my project.

Very special thanks go to Professors Fred Schwirzke and Alf Cooper for their overall assistance, encouragement, and guidance in producing this work. Last, but by no means least, I wish to thank my wife, who typed my early drafts and helped me organize my ideas.

This project was supported in part by funds from O.N.R.

I. INTRODUCTION

This work is the first phase of a project at NPS to study the characteristics, energy extraction techniques, and application to plasma production of a high power, short pulse, Iodine-photodissociation gas laser (PDL). This report concerns design, construction, and preliminary testing of an iodine laser oscillator. N-heptafluoropropyliodide (or perfluoropropyliodide) (C_3F_7I) gas buffered with argon is to be used as the lasing medium. Interest in this area stems from current work in progress at some of the major laboratories [3] around the world where the iodine laser is being studied in connection with laser fusion experiments.

A. BACKGROUND

The first laser pumped by photodissociation was developed by Jerome Kasper and George Pimentel at the University of California at Berkeley in 1964 [1]. Laser action was observed during flash photolysis of gaseous trifluoromethyliodide (CF_3I), and other alkyl iodide compounds. CF_3I was photolyzed in a wave band about 500 Å wide and centered about 2680 Å. Then stimulated emission resulted on the $^2P_{\frac{1}{2}} \rightarrow {}^2P_{\frac{3}{2}}$ magnetic dipole transition of atomic iodine. This transition corresponds to a wave length of 1.315 micrometers [1,4]. Kasper and Pimentel found that the photodissociation produced abundant excited iodine atoms in the $^2P_{\frac{1}{2}}$ excited state according to the

following reaction:

$$CF_3I + h\nu \rightarrow CF_3 + I(^2P_{\frac{1}{2}}). \qquad (1\text{-}1)$$

The forbidden transition from this excited state to the $^2P_{\frac{3}{2}}$ is

$$I(^2P_{\frac{1}{2}}) \rightarrow I(^2P_{\frac{3}{2}}) + h\nu_{laser} \qquad (1\text{-}2)$$

$$\lambda_{laser} = 1.315\,\mu m$$

Although previous works had dealt with similar compounds (e.g., CH_3I) [5], no studies had been made for photolysis of CF_3I. Kasper and Pimentel observed that the laser output is dependent upon the pressure of the lasing medium and that strong quenching occurs which terminates the reaction before full energy is extracted from the laser. A short time following their first paper, Kasper, Parker, and Pimentel reported that abrupt laser quenching prior to termination of the pumping flash is due to an increase in temperature [6]. They found that by lowering flash energy, quenching is prevented. Furthermore, they discovered that the addition of an inert buffer gas,(argon or C_2F_6), prevents low temperature quenching. However, they noted also that the introduction of I_2 vapor into the lasing medium increases the quenching problem.

Iodine laser output as a function of pressure in the lasing medium was measured by Pollack [2] in 1965. He offered a theory to account for this dependence. According to Pollack:

> "The decay of the atomic iodine population is due almost entirely to recombination into iodine molecules in a three body process. The lifetime, Γ^{-1}, typically tens

> of microseconds, depends on the pressure of atomic iodine and the pressure and nature of the "third body" species. Molecular iodine is a very effective third body and Γ increases as more I_2 is formed... In addition to photodissociative decay the undissociated molecules possibly decay through temperature dependent chemical reactions...." [2]

The decay rate he discussed is given by

$$\Gamma = N\Sigma_i k_i n_i \qquad i = 4, 5, 6 \qquad (1\text{-}3)$$

where k_i is the reaction rate of the i^{th} recombination process, n_i is the corresponding number of third body molecules, and N is the unsaturated effective inversion for the iodine. N is a function of the difference in statistical weights between the two states of iodine as well as time [2]. The relation (1-3) for the decay rate of iodine is a composite which includes the reaction rates of all the dynamic processes in the entire reaction.

Later, Kasper et al. [1,6] and Zalesskii and Venediktov [7] suggested that rapid heating of the laser gas results from collisional deexcitation when an iodine laser is pumped to produce the $I(^2P_{\frac{1}{2}} \rightarrow {}^2P_{\frac{3}{2}})$ transition. At high temperatures the controlling process becomes thermal dissociation rather than photodissociation. In thermal dissociation only unexcited iodine atoms are formed. This thermal dissociation process is known as pyrolysis.

Zalesskii and Moskalev in 1969 [8] reported having optically probed into the processes attendant to laser action. A pulsed beam of monochromatic light was focused through a narrow pass filter and into the iodine lasing medium, and

photon absorption was measured as a function of temperature. The probing radiation was in the form of a flat-top pulse up to 200-400 μsec long in a narrow band (20 to 40 Å) within the absorption region of Iodine (∿ 2600 Å through 3000 Å). The light passing through the active medium carries information about (1) variation in concentration of the working gas molecules (pyrolysis and photodissociation); (2) heating of the active medium resulting in deformation of the absorption band; (3) new products capable of absorption in this region of the spectrum. The experiment showed that pyrolysis occurs when heating of the active medium is sufficiently rapid. The temperature dependence of the recombination rate k_4 of the process is proportional to $\exp(-E_a/RT)$ where E_a is the activation energy and is reported to be close to the free energy ΔH of the pumping reaction ($\Delta H \simeq 57 \frac{kcal}{mole}$ @ 400° K), R is the universal gas constant, (R = 1.9872 cal/(mole deg)), and T is the kelvin temperature. Formation of molecular iodine was also found to occur. The experiment was significant in that it showed quenching in CF_3I occurs concurrently with the onset of pyrolysis. However, it was established that the addition of a sufficient quantity of argon to CF_3I (10:1) prevented the "pyrolytic" temperature from being reached. The pyrolytic temperature is given by

$$T_{cr} = E_a/R \ln (A/2\gamma) \qquad (1\text{-}4)$$

where A is the Einstein coefficient ($A = 10^{13} sec^{-1}$) and
is the coefficient of the exponential term in the decay rate expression ($k(T) = A \exp (E_a/RT)$)

γ is the probability of photodissociation

($\gamma(T) \sim 3 \times 10^{-3}$ sec^{-1})

E_a is the activation energy ($E_a \simeq \Delta H \simeq 57$ kcal/mole @ 400°K)

Inserting the given numbers in equation (1-4), one arrives at $T_{cr} \simeq 820°K$ which is born out by Zalesskii [8]. γ is a function of temperature and time. The addition of Argon gas to CF_3I slows the rate of temperature increase in the lasing gas so that the critical temperature is approached more slowly. Quenching due to pyrolysis is thus delayed.

Pollack [2] found that the use of a larger molecule C_3F_7I yields twice the energy that CF_3I yields. Zalesskii and Moskalev [8] confirmed Pollack's finding. They concluded that there is a significant difference in the degree of pyrolytic decomposition of C_3F_7I compared to CF_3I. This means there is less "wear" on the lasing gas when C_3F_7I is used. Furthermore, the low degree of working gas decomposition is probably due to the larger (by a factor of 2) thermal capacity of C_3F_7I ($C_{V_{C_3F_7I}} \simeq 34$ cal/mole; $C_{V_{CF_3I}} \simeq 17$ cal/mole). The C_3F_7I molecules have a larger physical size and therefore a higher photon-absorption cross-section. They exhibit the pyrolytic effect at a higher degree of dissociation of working gas than does CF_3I.

In 1974, Skorobogatov et al. [9] also studied the photolysis reaction which occurs in perfluorinated-propyliodide (C_3F_7I) compounds. In the study they calculated the recombination rate k_4 (eqn 1-3) for the recombination reaction using C_3F_7I (eqn 1-8). They further discovered the quenching mechanism

in CF_3I to be a temperature dependence of the rate constant in the recombination reaction. At photon flux densities greater than 10^{22} photons/cm^2-sec, in the iodine absorption band, the temperature of the working gas goes as high as 600 to 800°K. In this range the reaction rate k_4 for the recombination reaction forming CF_3I is 100 times greater than k_6 for the reaction in which I_2 (eqn 1-10) is formed [9]. As shown earlier, T_c at which onset of pyrolysis occurs is about 800°K.

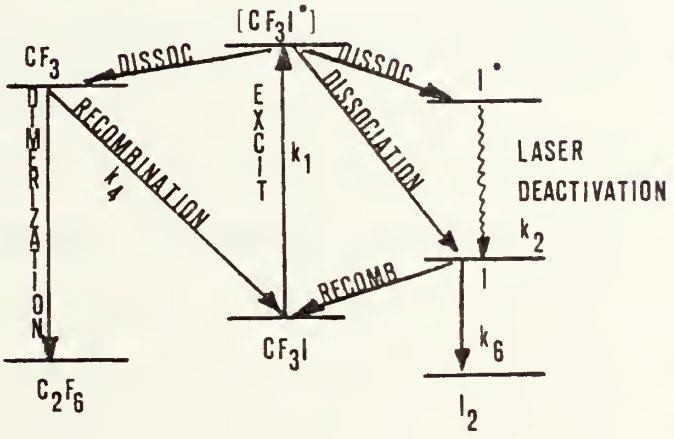

FIG. 1. Schematic Representation of the Typical Dissociation, Recombination and Lasing Processes in CF_3I.

Therefore, the increased rate of recombination near the onset temperature of pyrolysis depopulates the excited state faster than it can be pumped, and lasing ceases. See Figure 1.

One solution to quenching is to lower input flash energy. But that lowers the power output. As mentioned before, another solution is to add a buffer gas, argon, to prevent pyrolysis, and to use the larger molecule, C_3F_7I. This molecule is particularly suitable because it has almost complete

reversibility for the photodissociation process [14]. Hohla and Kompa have reported [14] up to 100 shots per fill using C_3F_7I-Ar as their working gas.

Present work uses almost exclusively perfluorinated propyliodide compounds as a laser working gas. It has been reported [10,11] that because of the long lifetime (170 ms) in the metastable state I ($^2P_{\frac{1}{2}}$), iodine would be well suited to giant pulse laser operation. It has been shown [14] that conditions can be found where there are no chemical limitations to the accumulation and storage of sizeable densities of excited iodine atoms.

Energy output of the oscillator is a pulse whose length depends on the number of frequencies contained in it. The pulse length is a function of the bandwidth of the laser transitions. Zeuv et al. [10] resolved the iodine luminescence spectrum into six hyperfine structural components. The luminescence line width, when any gas is under pressure, is governed by doppler and collision broadening. Under pressure, the sharp well-defined line of natural width no longer exists. The greater the pressure of a gas at a given temperature, the more frequent become the collisions between atoms. At high pressures spectral broadening becomes increasingly more dependent on molecular collisions. Zeuv et al. [10] and Hohla et al. [18] reported that at C_3F_7I pressures greater than 20 torr, pressure broadening dominates doppler broadening. Thus, laser output bandwidth becomes directly proportional to laser gas pressure. The minimum possible pulse length is a function of

the range of frequencies (i.e., bandwidth) present in the laser transitions and is therefore directly proportional to laser gas pressures greater than 20 torr (Fig. 2, 3). Thus, pulse width can be regulated in the iodine laser by addition of a buffer gas such as argon to the working gas to build pressures to greater than 20 torr. With increasing gas pressure, the atomic transition linewidth increases, thus increasing the range of possible laser frequencies in the output pulse.

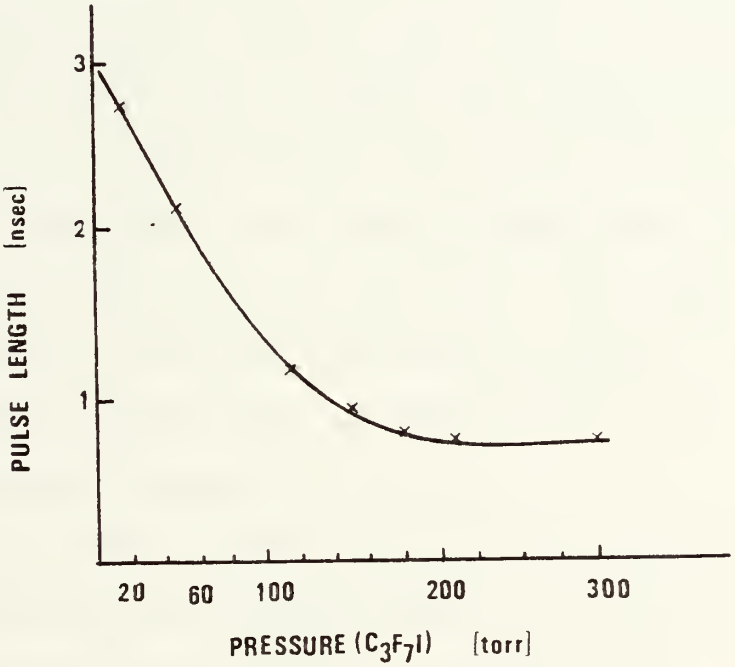

FIG. 2. This curve shows Pulse Length as a Function of Laser Gas Pressure [18]

One of the major problems presently confronting experimenters is how to extract more energy from the iodine laser in its pressure-controllable short pulse mode. In 1972 Hohla and Kompa [14] speculated that a scheme for pulse compression in the amplifier chain might result in very nearly full extraction of stored energy from the laser. These results

could be accomplished by operating the first amplifier in an "overshoot" region which is explained by Hohla and Kompa [14] as follows: "This type of operation is possible with fast pumping and judicious control of optical feedback: The inversion is increased above threshold by fast pumping, and the oscillator pulse is switched on before self-oscillation reduces population inversion." In this scheme, amplifier gain can be increased at the top of "overshoot," thus lowering the input energy required for saturation. Using a first stage of amplification operated in this "overshoot" region with a gain of 200, and a second stage pumped more slowly with a gain of 6, experiments performed by Hohla and Kompa [14] showed that almost all energy pumped into the excited atoms of the laser could be extracted. They speculated that an entire chain of amplifiers operated in the "overshoot" region would probably avoid the need for optical isolators between amplifier stages.

Recently, Jones, Palmer, and Franklin reported [13] on a new iodine laser oscillator operating with a 150 pico-second pulse length and 5 millijoules of output power. The oscillator is simultaneously Q-switched and mode locked and the flashlamps are discharged in parallel to eliminate magnetic field effects in the lasing medium. The laser is operated at a high pressure (1000-6000 torr) using C_3F_7I-Ar mixture with the C_3F_7I partial pressure held constant at less than 125 torr.[1] The use of

[1] It was observed that energy content of the output pulse is proportional to the amount of C_3F_7I contained in the lasing gas indicating that the mixture is optically thin to flashlamp pumping. But at C_3F_7I partial pressure greater than 125 torr the energy content of the output pulse decreases with total pressure increase. [13]

high pressure exploits fully the adjustable pulse length feature of the iodine laser as a function of gas pressure (Fig. 3). It is expected that pulses of approximately picosecond width and peak energies of 10^4 joules are required to produce "break-even" laser fusion reactions. Some observers feel that the iodine laser will suit this requirement.

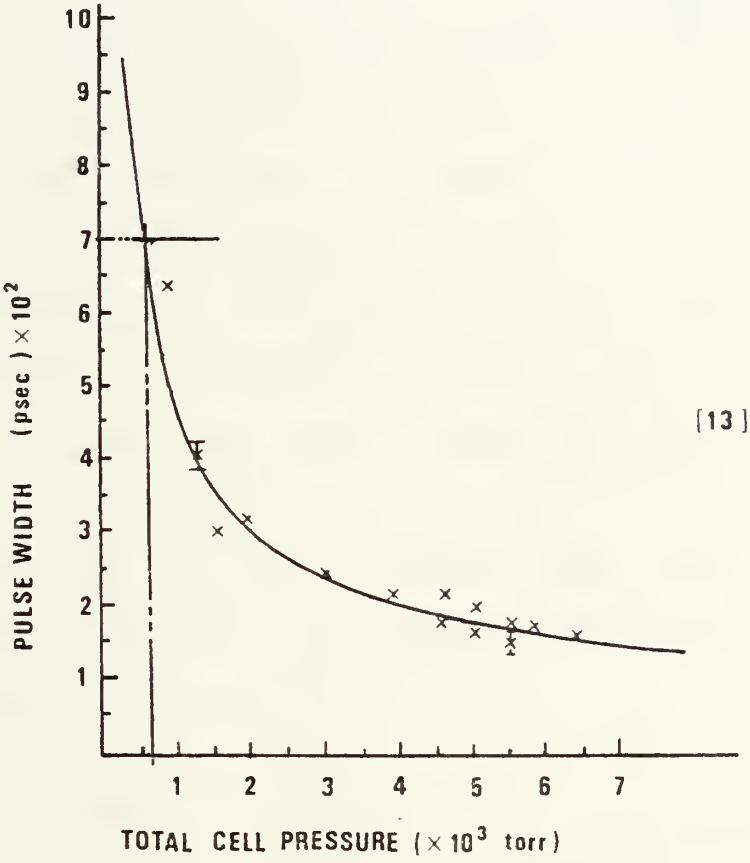

[13]

FIG. 3.

Optical pumping in most of the existing iodine laser systems is accomplished by discharging a high current through a xenon flash tube. Other schemes have been tried with good results. In 1974, Silfvast, Szeto, and Wood succeeded in pumping an iodine laser with ultraviolet light from a xenon plasma produced by a pulsed CO_2 laser. They compared this scheme to the usual flashlamp pumping method and reported

[16] that for the same input energy the laser-produced plasma pumping scheme produces a shorter, sharper-rising laser output at λ = 1.315 μm than does the flashlamp scheme. In the study the output from a TEA CO_2 laser was focused onto an aluminum target inside a cell filled with xenon gas. A plasma was formed in the xenon gas adjacent to a quartz tube containing C_3F_7I. A polished aluminum sheet wrapped around the quartz tube acted both as a target for the CO_2 laser and as a collector for the UV radiation. For comparison, a flashlamp with approximately the same dimensions as the laser-produced plasma was mounted adjacent to the quartz tube and discharged via an electrical pulse of comparable duration to the CO_2 laser pulse. Both the CO_2 laser pulse and the electrical discharge pulse had the same energy input per unit length. The radiative outputs from both the laser-produced plasma and the electrical discharge were monitored. The laser-produced plasma/flashlamp pumping scheme is shown in Fig. 4.

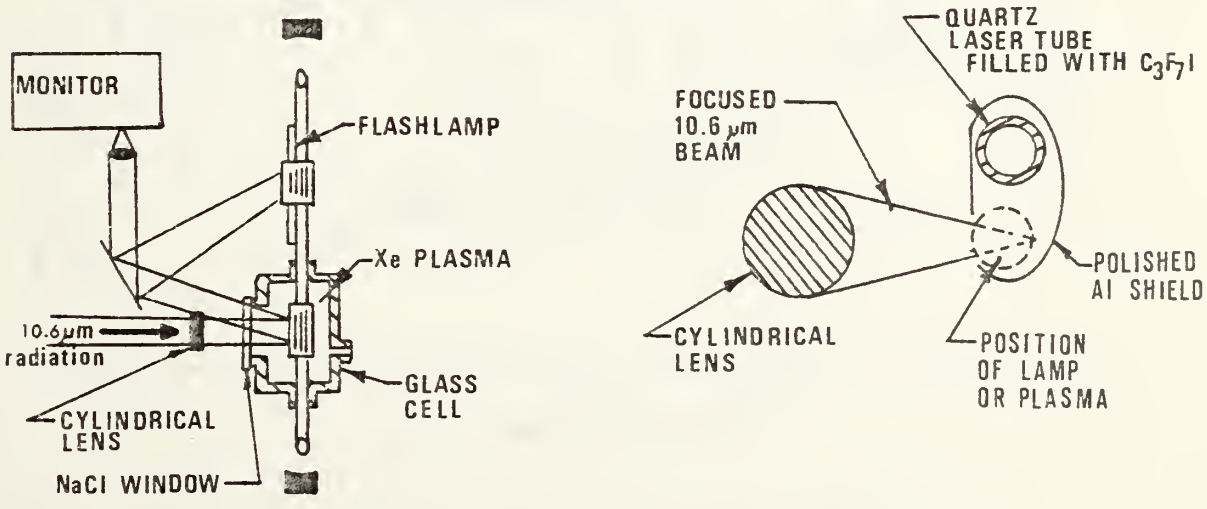

FIG. 4. Scheme for Comparing Photodissociation by Flashlamp with that Produced by Radiation from Laser-Produced Plasma. [16]

Silfvast and Wood had investigated the heating of a xenon plasma in an earlier work [20]. They discovered a vast difference in the spectral radiance curves (Figure 5) in the range of wavelengths from 250 to 350 nm when the xenon plasma was produced by a laser instead of an electrical discharge. Iodine is pumped in this band. So when Silfvast, Szeto, and Wood [16] later experimented with the CO_2 laser-produced plasma to pump an iodine laser, they expected to find greater intensity in the output pulse. Their expectations were confirmed.

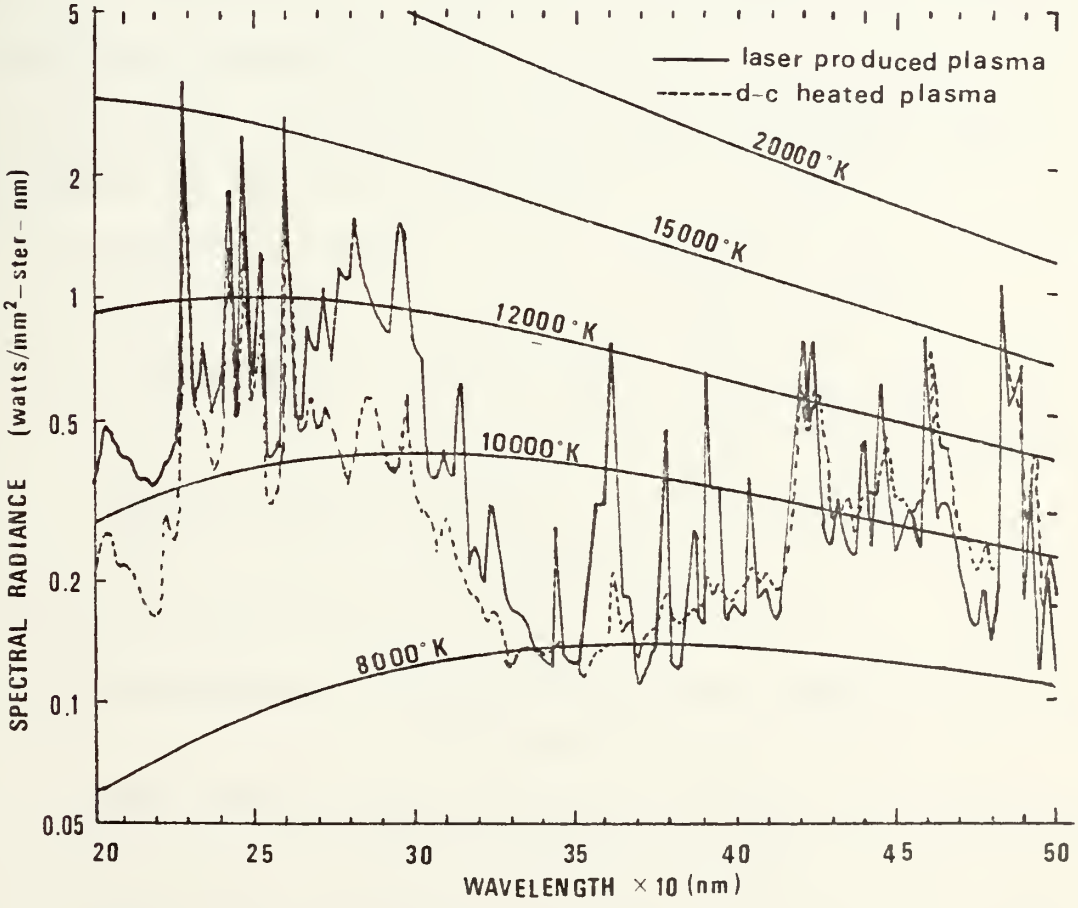

FIG. 5. Spectral radiance as a function of wavelength produced by 0.8-J/cm input energy for a laser-produced plasma (50 Torr Xe) and a dc-heated plasma (400 Torr Xe). [20]

Another alternate method of pumping was reported by Basov et al. [27, 28, 29] and Anatov et al. [19]. They described an amplifier designed for short pulse, high power operation, and pumped by the light from an exploding tungsten wire. The pumping radiation is derived from the thermal wave of an electric discharge in an active substance. Large currents ($\sim 10^3$ amps) are passed through a fine ($\sim$ .1 mm) tungsten wire. The wire explodes, resulting in an intense light source. Anatov et al. [19] claim they have been able to achieve output energies of over 700 Joules from an amplifier 1.5 m long with a diameter of 36 cm when itis pumped with an exploding tungsten wire.

The criteria we hope to achieve in the iodine laser oscillator at NPS are as follows:

Oscillator output - - - - - $\sim$ 5 mJ

Pulse (FWHM) - - - - - - - - $\sim 10^{-9}$ - 10^{-8} sec.

Flash duration (preionized) $\sim$ 10-100 μsec.
$\leq$ 10 μsec in pumping range

Pumping energy available - $\sim$ 300 Joules
(Cap. 1.5 μf @ 20,000 volts)

We are using the following:

Lasing medium: C_3F_7I @ 20-70 torr (approx.) buffered with argon to C_3F_7I (10:1-60:1)

Flash tubes: Quartz 58.42 cm (23 in.) in length with 26 cm (10-1/4 in.) used to pump the laser

Laser tube: SUPRASIL, 26 cm (10-1/4 in.) in length ID = 5 mm (.204 in.)

Brewster windows: quartz n = 1.6, $\theta_b \sim 57°$

Resonator: It is hemi-confocal with a length of 86.4 cm (34 in.); the spherical mirror has a radius of 1.5 m (59.05 in.) and is gold coated (3000 Å) with a reflectance of $r \geq 98\%$; the planar output mirror is a gold coated (110 Å) quartz window with a reflectance of $r_2 \simeq 75\%$.

B. THEORY

1. Reaction Kinetics

The iodine laser is a photochemical dissociation laser. Ultraviolet light around 2700 Å from xenon-filled electrical flashlamps is used to dissociate an organic iodine compound, namely, n-heptafluoropropyl-iodide (C_3F_7I). The photochemical dissociation process results in the formation of neutral atomic iodine in the $5p^2\ {}^2P^{\circ}_{\frac{1}{2}}$ excited state by the absorption reaction

$$C_3F_7I + h\nu_{uv} \xrightarrow{k_1} C_3F_7 + I({}^2P^{\circ}_{\frac{1}{2}}) \qquad (1\text{-}5)$$

with reaction rate k_1. The excited state is radiatively coupled to the ground state ${}^2P_{\frac{3}{2}}$ via a magnetic-dipole transition and the spontaneous emission of a photon at a wavelength of $\lambda = 1.315$ μm with a reaction rate k_2 in the reaction

$$I({}^2P_{\frac{1}{2}}) \xrightarrow{k_2} I({}^2P_{\frac{3}{2}}) + h\nu \qquad (1\text{-}6)$$

The radiative lifetime of the excited $I({}^2P_{\frac{1}{2}})$ state has been reported to be in the range $125\ \text{ms} < \tau_R < 170\ \text{ms}$ [10, 11, 16]. Because of this long metastable lifetime, virtually all the dissociated atoms are left in an excited state. Therefore, a

large population inversion can be established by ultraviolet pumping which has a shorter duration than the lifetime in the upper state.

The concentration of atoms in the upper state is influenced by a secondary chemical reaction during and after the flash. The atoms lose excitation by stimulated emission with rate constant k_3 according to

$$I(^2P_{\frac{1}{2}}) + h\nu_{laser} \overset{k_3}{\rightarrow} I(^2P_{\frac{3}{2}}) + 2h\nu_{laser}. \quad (1\text{-}7)$$

Then, recombination with a reaction rate k_4 reestablishes the lasing medium by

$$I(^2P_{\frac{3}{2}}) + C_3F_7 \overset{k_4}{\rightarrow} C_3F_7I. \quad (1\text{-}8)$$

Collisional de-excitation occurs with a reaction rate k_5 according to

$$I(^2P_{\frac{1}{2}}) + C_3F_7I \overset{k_5}{\rightarrow} I(^2P_{\frac{3}{2}}) + C_3F_7I \quad (1\text{-}9)$$

followed by collisions according to

$$2I(^2P_{\frac{3}{2}}) + C_3F_7I \overset{k_6}{\rightarrow} I_2 + C_3F_7I \quad (1\text{-}10)$$

which leads to the formation of molecular iodine.

A system of equations was derived by Kamarov et al. [17] to describe the dynamics, the time evolution of the concentrations of $[CF_3I]$, $[I(^2P_{\frac{1}{2}})]$, $[I(^2P_{\frac{3}{2}})]$, $[CF_3]$ and the intensity of the stimulated emission transition for CF_3I as a working gas. They were extended by Skorabogatov et al. [9] to calculate the reaction rate constants k_i ($i = 1$ through 6) and other important kinetic characteristics of the iodine

laser, using C_3F_7I. They assumed that prior to peak laser energy output at t_{max}, only equations (1-5) through (1-8) occurred in a working volume of C_3F_7I gas. By solving a system of chemical reaction rate equations, they arrived at a relation for the differential quantum yield of stimulated emission ($\Gamma_\Sigma(\%)$) as a percentage of the theoretical maximum possible value of two-thirds of the particle number n, given by the initial pressure. $\Gamma_\Sigma(\%)$ expressed in terms of measured stimulated-emission energy per cm^3 of the working volume (E_{gen}) is

$$\Gamma_\Sigma(\%) = \frac{0.988 \times 10^{19} E_{gen}[J/cm^3]}{n\ [molecules/cm^3]} \cdot 100 \quad (1\text{-}11)$$

The maximum possible value of stimulated-emission energy per volume is then:

$$\Gamma_\Sigma = (2/3n) \int_o^{t_{cut}} G(t)\, dt \quad (1\text{-}12)$$

where n is the initial pressure of C_3F_7I (molecules/cm^3)

G(t) is intensity of stimulated transitions (photons/cm^3 sec)

t_{cut} is time of termination of generation of excited atoms (sec) (i.e., quenching, etc.).

By using measured values of lasing energy, E_{gen} and laser pulse shapes (Fig. 6), the maximum power of stimulated emission per working volume, E_{max} (J/cm^3 sec), can be calculated for peak laser output at time t_{max}.

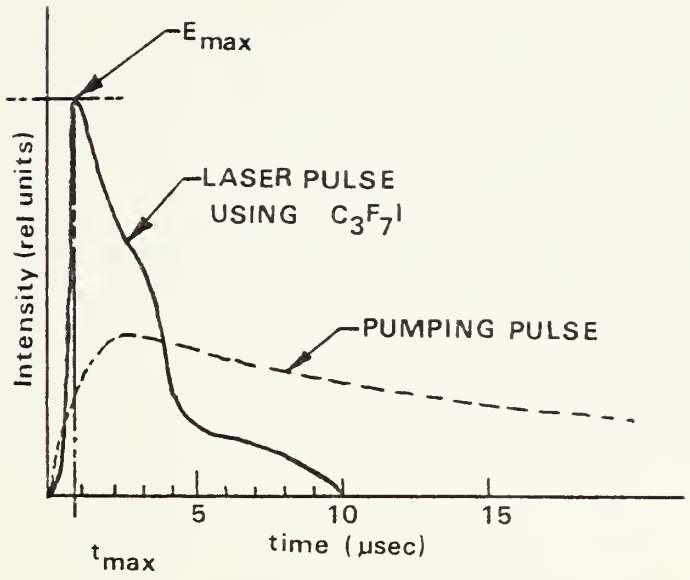

FIG. 6. Typical pulse shape with measuring points E_{max} and t_{max} indicated.

Assuming a pumping photon has an energy of 3.6 ev for C_3F_7I [9], and by putting E_{max} in terms of photons/cm^3 sec, (G_{max}), the apparent pumping radiation flux in the iodine absorption band at the time of peak output (t_{max}) can be calculated [9].

$$\phi_{max}^{C_3F_7I} \text{ [photons/cm sec]} = \frac{1.5\ G_{max}\ \text{[photons/cm}^3\ \text{sec]}}{n\ \sigma(p)\ [\mathcal{R}I]} \qquad (1\text{-}13)$$

where n is the initial pressure of C_3F_7I

$\sigma(p)$ is the stimulated emission cross-section of the C_3F_7I molecule as a function of pressure

$\phi_{max}^{C_3F_7I}$ is the apparent flux or actual pumping flux [9,17]

$\mathcal{R}$ is the radical C_3F_7 or CF_3.

It was shown by Skorobogatov [9] that calculations made for the iodine laser using CF_3I as a working gas could

be applied to a laser using C_3F_7I. Maximum laser output occurs at the same time (t_{max}) in both gases for a given pump energy and pressure. Therefore, the stimulated-emission energy yield $\Gamma_\Sigma(t_{max})$ for C_3F_7I goes as the ratio of the fluxes $\phi_{max}^{C_3F_7I}/\phi_{max}^{CF_3I}$ at the time of peak output. Some values for $\phi_{max}^{CF_3I}$ have previously been calculated [17] and tabulated (Figure 7). Then, for a laser using C_3F_7I the laser peak energy output at the time t_{max} can be found by

$$\Gamma_\Sigma^{C_3F_7I}(t_{max}) = (\phi_{max}^{C_3F_7I}/\phi_{max}^{CF_3I})\Gamma_\Sigma(t_{peak}) \qquad (1\text{-}14)$$

2. Energy Storage

As mentioned earlier, the bandwidth of the output pulse of the iodine laser can be controlled by the pressure of the working gas in the laser cell. Ideally, for laser fusion, one would like to extract the entire energy in the shortest possible output pulse. In order to develop the power in a short pulse from an amplifier, the medium must have a simulated-emission cross section low enough to prevent premature spontaneous laser action, equation (1-6) [22].

Stimulated emission cross sections can be lowered by broadening the laser emission linewidth. Two methods have been used successfully to increase the distance between the hyperfine levels of atomic iodine and thus broaden the linewidth.

Gensel, Hohla and Kompa reported in 1971 [3] the use of an inhomogeneous magnetic field to increase the hyperfine level separation and thus the energy storage capability of

(CF_3I) torr	n mole/cm^3	E_{pump} J	E_{las}, mj/cm^3	t_{max}, μsec	t_{quen}, μsec	Γ_Σ (%)	$G_{max} \cdot 10^{-23}$ photon/cm^3 sec	$\eta(t_{max})$
15	$4.9 \cdot 10^{17}$	40500	1.22	200	1400	2.31	0.0009	0.995
20	$6.6 \cdot 10^{17}$	--	--	15	50	5.2	--	0.956
22	$7.2 \cdot 10^{17}$	3420	4.6	0.5	5	6.21	1.39	0.986
37	$1.22 \cdot 10^{18}$	1840	5.0	--	20	4.01	0.163	0.987
		1520	13.5	2.5	20	5.46	1.10	0.984
74	$2.44 \cdot 10^{18}$	855	15.1	1.0	10	6.11	3.35	0.979
		1840	15.4	1.8	9	6.2	4.64	0.950
		2570	15.4	1.0	5	6.2	5.76	0.965
100	$3.29 \cdot 10^{18}$	--	--	38	73	4.3	--	0.934
111	$3.65 \cdot 10^{18}$	1840	14.8	--	20	4.01	0.488	0.987
		2375	23.9	4.0	27	3.86	1.41	0.986
185	$6.1 \cdot 10^{18}$	1840	30.5	1.5	7	4.94	9.16	0.967
		2570	35.1	1.5	6	5.68	10.02	0.964
		1600	21.4	4.0	16	1.73	1.80	0.991
370	$1.22 \cdot 10^{19}$	2280	27.0	2.5	13	2.19	2.12	0.993
		3420	39.9	2.0	5	3.23	14.7	0.965

FIG. 7. Tabulation of Laser Characteristics for a CF_3I Laser [17]

the laser. They concluded that chemical composition in the laser tube and control of the linewidth could improve energy extraction from the laser. Zeuv et al. extensively investigated the hyperfine structure of atomic iodine [10]. In Figures 8 and 9 the hyperfine structure and the transitions for atomic iodine are shown. The F=3 to F=4 transition is the most intense and the one observed in most laser experiments [12,15]. The transitions F=3 → 3 and F=2 → 2 have nearly the same line strength. However, F=3 → 3 is not observed in the absence of a magnetic field. The absence of this transition implies that relaxation among the hyperfine sublevels of $I(^2P_{\frac{3}{2}})$ is rapid compared to the time scale of laser emission [15]. The F=2 → 2 transition is sometimes completely absent, indicating that it is barely above threshold. This is attributable to rapid relaxation between the hyperfine sublevels of the excited $(^2P_{\frac{1}{2}})$ level [15].

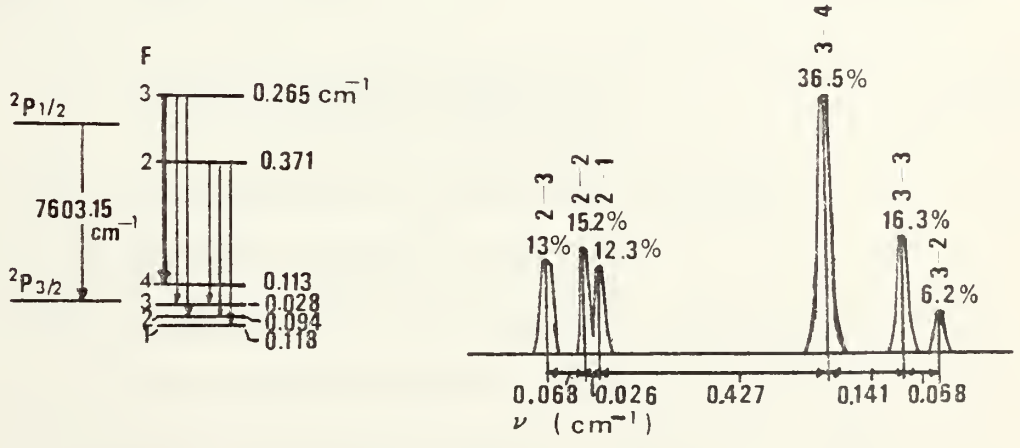

FIGURES 8 & 9. Hyperfine Splitting of the Iodine Laser Transition at C_3F_7I Pressure of 15 torr [10]

Line width is governed by doppler and collision broadening as a function of gas temperature. Relative positions of the lines are shown in Figure 9. According to Zeuv et al. [10], the doppler width (W) does not depend on density of the gas, but the collision width (γ) varies in proportion to density.

In experiments [10] done with C_3F_7I mixed with argon (at 1:18), at total pressure of 300 torr the luminescence line is broadened mainly by collisions. The collision width can be calculated. Assuming a Vander-Waals interaction of atomic iodine with argon, collision line width is given by

$$\gamma = 8.16\ NC^{\frac{2}{5}}\ \bar{V}_{th}^{\frac{3}{2}} \qquad (1\text{-}15)$$

where N is the concentration of perturbing particles ($\sim 10^{19}\ cm^{-3}$ @ 300 torr) and $\bar{V}_{th} \sim 400$ m/sec is the average relative velocity of colliding particles. The constant C is expressed in terms of the polarizability of the interacting particles α_1, and α_2 [10].

$$C = 3/(2\hbar)\frac{\sqrt{a_o}\ e^2\ \alpha_1\ \alpha_2}{\sqrt{\alpha_1/N_1} + \sqrt{\alpha_2/N_2}} \qquad (1\text{-}15a)$$

where $\hbar$ is the constant ($1.05499\ 10^{-34}$ J-sec)

a_o is the Bohr radius (0.5292 Å)

α_1 is polarizability of argon ($1.6 \times 10^{-24}\ cm^3$) [10]

α_2 is the estimated polarizability of $I(^2P_{\frac{1}{2}})$

e is the electronic charge (1.602×10^{-19} coul)

N_1 is the number of electrons in argon (18)

N_2 is the number of electrons in iodine (53).

From photographs of the spectrum of excited iodine one can determine the line width γ. Using equations (1-15) and (1-15a) the polarizability of atomic iodine in $I(^2P_{\frac{1}{2}})$ excited state can be calculated. Zeuv et al. [10] in experiments using the above conditions reported a value for the line width due to collision broadening to be

$$\gamma = 0.060 \pm 0.012 \text{ cm}^{-1}$$

The total true luminescence line width of atomic iodine is a function of the pressure of the buffer gas. The pressure controls the collision broadening γ as a function of the density and the temperature of the gas averaged over the length of the working cell volume. The gas temperature controls the doppler broadening. It is negligible when C_3F_7I and argon is used as a lasing medium. Hohla and Kompa in 1973 suggested [14] broadening the iodine emission line by adding inert gas to the lasing medium. Their experiments showed that hyperfine levels could thus be widened without using a magnetic field. When partial pressures of the inert gas exceed 20 torr, the line width increases as a function of pressure. This is pressure broadening. Brederlow, Hohla, and Witte determined [23] that energy stored in an iodine laser cannot be fully extracted. As a consequence of the degeneracy of the upper and lower levels of iodine and owing to homogeneous pressure broadening of all the hyperfine components, a maximum of 66% of the stored energy could be extracted. To see the relation of energy storage to pressure, one must look first to laser gain.

Prior to the occurrence of lasing, a resonant optical cavity acts like an amplifier. Pumping energy is stored by excited atoms in a population inversion. When the atoms transition to lower states they radiate at certain frequencies. When the frequencies are compatible with the resonant cavity, amplification occurs. Like any resonant oscillator, the laser can be characterized in terms of gain, internal loss and useful output. When the gain for a suitable frequency in the laser cavity exceeds the losses incurred by the wave as it moves between the mirrors of the cavity, lasing occurs. From this point on, the cavity ceases to amplify and becomes an oscillator. The point at which oscillation is achieved is known as threshold. Gain of the laser medium is given by

$$G_{th} = \exp(\sigma \Delta n L) \qquad (1\text{-}16)$$

where σ is the stimulated emission cross section

Δn is the population inversion

L is the length of the laser medium in the light path

The product $(\sigma \Delta n)$ is called the gain coefficient.

If population inversion and length of the active medium are known, one can calculate the stimulated emission cross section (σ). However, there is an easier way. The gain given by equation (1-16) can be related to mirror reflectances as follows:

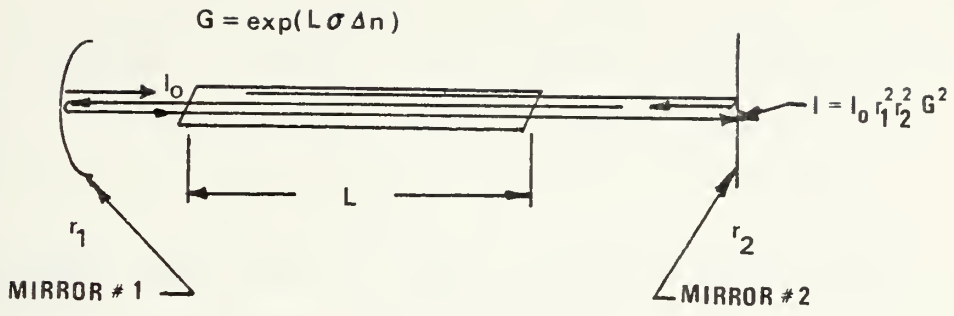

FIG. 10. Typical Laser Cavity

Consider the situation pictured in Figure 10 where light of some intensity, I_o, and some frequency, ν, near the laser transition, enters a suitable laser cavity. Each time the light passes through the laser medium it will experience a gain given by equation (1-16). At mirror #2 after the first pass the intensity is

$$I = I_o \exp(L\sigma\Delta n) \tag{1-17}$$

After reflecting from both mirrors, the light intensity returning to mirror #2 is given by

$$I = I_o r_1^2 r_2^2 \exp(2L\sigma\Delta n) \tag{1-18}$$

where r_1 and r_2 are the reflectances of mirrors #1 and #2 respectively. When gain threshold is reached, lasing occurs, and pumping energy additionally delivered to the laser is no longer stored. It is converted directly, by the laser medium, into radiation with the laser frequency. Therefore, the lasing criterion demands the amplifier gain equation (1-18) to become

$$I = I_o r_1^2 r_2^2 G^2 \tag{1-19}$$

After lasing occurs, energy is no longer stored, so $I=I_o$. Then, assuming no internal scattering loss, equation (1-18) becomes

$$G_{th} = 1/r_1 r_2 \qquad (1\text{-}20)$$

By choosing values for r_1 and r_2, gain threshold for the NPS laser can be predicted. Selecting $r_1 = .98$, $r_2 = .75$ and using (1-17)

$$G_{th} \simeq 1.36 \text{ [round trip]}^{-1}$$

By increasing the reflectance r_2 the value of the threshold gain can be lowered. Knowledge of the gain per pass allows determination of the gain cross section σ.

Stimulated emission cross section (gain cross section) σ is found using equation (1-16). Then the line width in terms of frequency difference can be found. Zeuv et al. [10] and Paderick and Palmer [24] assumed a lorentzian shape for the distribution of light frequencies in the output energy spectrum. The lorentzian line width is related to the stimulated emission cross section (gain cross section), σ, as follows [26]

$$\Delta\nu = \frac{Ac^2}{8\pi\nu^2\sigma} = D = \frac{A\lambda^2}{8\pi\sigma} \qquad (1\text{-}21)$$

where $\Delta\nu$ or D is line width (FWHM)

λ is wavelength in cm

A is radiative decay rate (Einstein coefficient [sec^{-1}])

σ is the stimulated emission cross section [cm^2]

c is the speed of light ($c = \lambda\nu$)

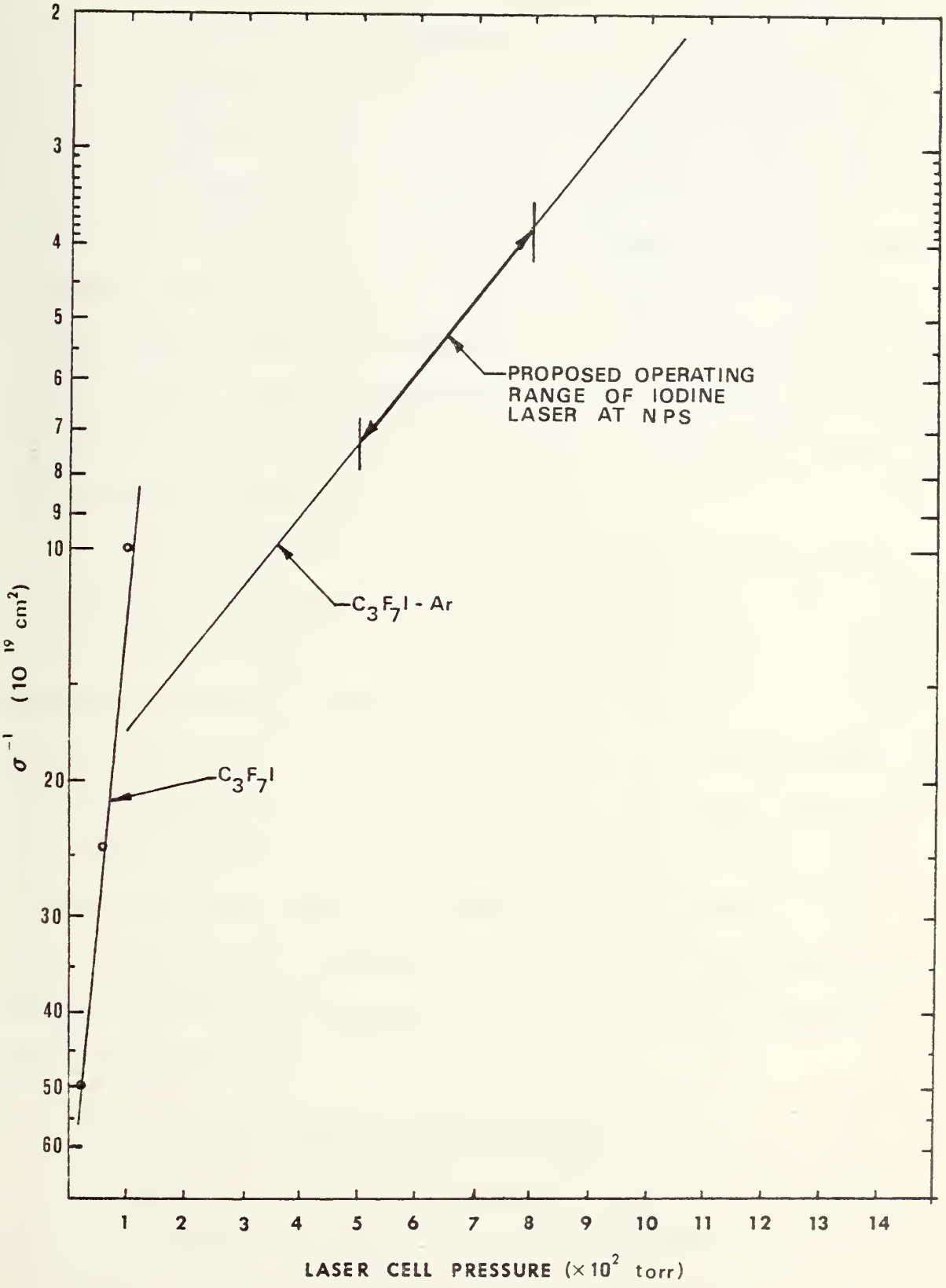

FIG. 11. Stimulated Emission Cross Section as a Function of Pressure [25]

Values for the stimulated emission cross section (gain cross section) σ have been calculated ($10^{-19} \leq \sigma \leq 10^{-18}$ cm^2). [23, 24]. Figure 11 shows the relation between stimulated emission cross section and pressure. Thus, if the cavity mirror reflectances, the population inversion, and length of the laser medium are known, one can compute the stimulated emission cross section (σ). With knowledge of σ, the corresponding pressure requirements can be found as well as the line width, D, and the frequency distribution of the output spectrum. For the computation of line width, a knowledge of the Einstein coefficient is necessary.

The radiative decay rate or Einstein coefficient A is similar to the quantity called Γ in equation (1-3). Zeuv et al. [10] determined the total transition rate A_T for all the transitions in Figure 8 to be $A_T = 5.4$ sec^{-1}. They calculated the ratio of the $5P_{\frac{1}{2}} \rightarrow 5P_{\frac{3}{2}}$ (F=3 → F=4) transition rate to total transition rate to be 5/7.7. This ratio times rate A_T gives $A_{3-4} \simeq 3.5$ [transitions.sec^{-1}] for the $5P_{\frac{1}{2}} \rightarrow 5P_{\frac{3}{2}}$ transition. The transition rate A when inverted is the lifetime of the metastable state: ($\tau_L = A^{-1} \simeq 170$ ms) [10]. As can be seen, the lifetime of the population inversion is exceptionally long.

C. TRANSMISSION THROUGH THE ATMOSPHERE

The iodine laser is well suited for atmospheric transmission experiments. It can be seen in Figure 7 that its wavelength falls in a transmission window with a transmittance $\tau > 90\%$ over a 0.3-km path at sea level.

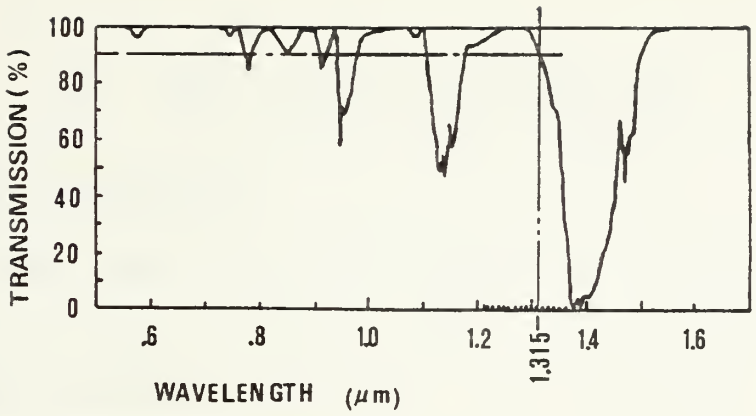

FIG. 12. Atmospheric Transmission Windows Over a .3-KM Path at Sea Level [21]

II. THE IODINE LASER OSCILLATOR

A. GENERAL DESCRIPTION

The iodine laser oscillator consists of a laser tube, two brewster window assemblies, and two parallel-mounted, xenon-filled, quartz flash tubes. The flashtubes have an arc length of 45.68 cm (18 inches) between the electrodes. The working laser cell is a Suprasil tube, 37.75 cm (14.57 in.) in length, with a 5 mm (0.197 inch) inside diameter, and walls 1 mm (0.039 inch) thick. The laser tube is set into two machined monel laser heads which are separated by 30.77 cm (12.125 in.). They are fitted with O-ring vacuum seals and are designed for a system base pressure of 10^{-5} torr. The brewster windows are 3.175 mm (0.125 in.) thick quartz glass and are flange-fitted and O-ring sealed to the monel laser heads. The C_3F_7I laser gas is transported from stainless steel holding tanks (WHITEY 500 cc sample cylinders) via 1/4 inch diameter stainless steel tubing. NUPRO Series 4BK stainless steel valves and SWAGELOK stainless steel fittings are used in the laser gas transport system. (It is expected that fluoridated iodine is corrosive to brass, aluminum, and copper. Thus, monel and stainless steel were chosen for their resistance to corrosion.) The buffer gas, argon, is introduced through 1/4 inch diameter nylon tubing. It passes through a series of isolating valves, a pressure transducer, and then into the laser gas system. The pressure transducer

measures absolute pressure by sensing the change in magnetic reluctance of a magnetic circuit caused by the displacement of a stainless steel diaphragm. The sensor is shown in Figure D-13. The output of the sensor is a d-c voltage which is measured by a d-c voltmeter. The calibration curves are shown in Appendix A.

Two auxiliary gas systems, one for xenon and one for nitrogen, are used with this laser. The xenon system provides the gas for the flashtubes, which are used to pump the laser. The other auxiliary gas system transports nitrogen which is used as an atmosphere in the four-element spark gap. By adjusting the pressure of the nitrogen in the spark gap, one can set the threshold voltage of the spark gap at any one of a wide variety of voltages. Both auxiliary gas systems can be operated independently of the main laser gas system. Both have pressure gauges built into them.

Energy input to the flashtubes is provided by discharging a capacitor bank by trigger command. A large discharge current from the capacitor passes via low inductance leads through the parallel-mounted flashtubes producing the pumping pulse of ultraviolet light. The capacitor bank is charged to 15-24 KV by a power supply capable of a maximum current of 50 ma. The spark gap is a four-element, pressurized spark gap identical to those described by Budzik [30]. The charging voltage is measured by placing a voltmeter in series with 150 megohms resistance across the terminals of the capacitor.

The stored energy in the capacitor bank, and thus the input energy to the flashtubes is given by

$$E = 1/2\ CV^2$$

where C is the capacitance in farads

V is the charging voltage in volts

E is the energy input in joules

B. ARRANGEMENT OF SYSTEM COMPONENTS

Figure D-2 shows the physical arrangement of the various components of the iodine laser oscillator and its supporting subsystems. Positioning of the components was dictated by space available, ease of access to the equipment, proximity to a large power source, and future expansion. The power supply and triggering system is the one used for the NPS theta-pinch bank [30]. Only a slight modification to the wiring in the triggering system was necessary to adapt the control system to the laser. The modification removed the remote firing capability used in the theta-pinch.

The oscillator was constructed mostly of equipment found about the laboratory. It was made adjustable in every respect to allow for experimental alteration of its size.

C. DATA

The following table lists the most important data for the iodine laser oscillator.

Parameters:	Measured Quantity:
Laser Volume	64.352 cm^3 (3.279 $in.^3$)
Charging Voltage	15-24 KV
Capacitance	1.5 μf
Capacitor Charge Time (5 time constants)	∿ 60 sec
Stored Energy (input)	∿ 169-432 J
Energy Effective in Photolysis	∿ .8 - 1.5 J
Flash Duration (measurable)	See Appendix H
Flash Pulse Rise Time (measurable)	
Laser Pulse Rise Time (measurable)	
Laser Output Pulse Length (measurable)	
Total Laser Energy Output (measurable)	

Rise time is defined as the time it takes the pulse to increase from 10% to 90% of its maximum value.

III. DESIGN AND CONSTRUCTION OF THE IODINE LASER OSCILLATOR

A. LASER GAS TRANSPORT/VACUUM SYSTEM

Figure D-1 is a schematic of the entire vacuum/gas transport and purification system. A VACUUM ELECTRONICS CORP. Model EP25W, 2-1/2 inch, air-cooled diffusion pump is used to achieve a system base pressure of the order of 10^{-5} torr. Complete isolation of the vacuum pump from the gas handling systems is accomplished by high vacuum valves. The laser gas transport system and the flashtube fill system are independent of each other although they can be connected to the same vacuum system. Diffusion pump inlet pressure is monitored by a VEECO, type RG-75, ionization gauge with a response range of 10^{-10} to 10^{-2} torr. In the range 10^{-2} to 1 torr it is measured by thermocouple. Gas pressure in the range of 1 torr to 760 torr is monitored by a NELSON vacuum gauge and also by a variable reluctance pressure transducer. The transducer measures absolute pressure by sensing the change in reluctance of a small magnetic circuit. The reluctance is proportional to the position of a stainless steel diaphragm. The sensing element generates a d-c voltage which is amplified by a BENTLEY CORPORATION model E-15 amplifier and monitored by a HEWLETT-PACKARD model 419A d-c null voltmeter. A calibration procedure and calibration curves for the transducer are shown in Appendix A.

In this laser, argon is used as a buffer gas and represents the major part of the laser working gas. The argon is introduced from a tank through metering valves 4 and 9 and into the main gas system. Absolute pressure of the argon is measured by the same pressure transducer used to measure the C_3F_7I.

B. LASER GAS PURIFICATION

The chemical used in the master oscillator as a lasing medium is C_3F_7I (Perfluoropropyl iodide, ALDRICH CHEMICAL CO., Inc.). It can be obtained at 99% purity. The main impurities in the gas as a result of the manufacturing process are oxygen (O_2) and carbon dioxide (CO_2) which must be removed prior to laser operation. The impurities may be removed by a vacuum trap-to-trap distillation process employing a cold bath. The boiling points for C_3F_7I, CO_2 and O_2 are, respectively, 41°C, -78°C, -183°C. The recondensing vessel and the C_3F_7I storage vessel are WHITEY 500 cc stainless steel sample cylinders. Each of the cylinders can be separated from the vacuum system by a valve, and the entire purification system can be isolated from the rest of the system by valves 1, 4, 7, 8. The purification process is described in Appendix C.

An additional impurity problem arises because C_3F_7I self-dissociates in storage, forming I_2 molecules. I_2 is a very effective quenching agent for excited iodine atoms and must be removed for successful lasing [6, 32]. Introduction of either silver wool or copper mesh into the C_3F_7I storage tanks

removes the I_2 by forming silver iodide or copper iodide respectively. In the iodine laser at NPS, 6-inch strips of copper mesh are deposited in the C_3F_7I storage tank to control the molecular iodine formation problem.

C_3F_7I is light sensitive. In order to prevent light from entering the cavity through the ends of the reflector assembly, heavy black paper is cut out of a pattern and placed over the reflector ends. This keeps light entry into the cavity to a minimum.

C. HIGH VOLTAGE POWER SUPPLY AND CONTROL SYSTEM

The high voltage power supply and control system employed in the iodine laser are similar to those used in the theta-pinch at NPS, as described by Budzik [30]. Modification has been made to the control system circuitry in order to adapt it to the iodine laser. For example, the laser uses only one capacitor instead of the six employed by the theta-pinch. The wiring for charging the master spark gaps as well as the remote control triggering feature for the theta-pinch has been disconnected from terminal board B at the local control station, and TB-8B was jumpered to ground to close the 115 VAC relay control circuit. All other wiring for the theta-pinch remains the same.

Figure D-3 shows the trigger control circuit for the iodine laser oscillator. The control circuit performs three functions: 1) Charging the capacitor and spark gap, 2) dumping the capacitor and spark gap, 3) discharging the capacitor through the parallel-mounted xenon-filled flashtubes.

Figure D-4 shows the relay logic for the control system functions. K8A and K9A are contacts of vacuum relays K8 and K9 located in the large 50 KV power supply. They are the key components of system control. K8A is normally closed, thus preventing the capacitor from collecting a lethal charge. K9A is normally open and is used to charge the capacitor and spark gap. The 25 KV circuit is used to charge the capacitor up to threshold voltage for the flashlamps. When the charge button is pushed, K8A opens, K9A closes, and charging begins. When the dump button is pushed, K9A opens, followed by the closing of K8A, and the capacitor is shorted to ground. The switching sequence mentioned here is built into the power supply. It is important because it prevents shorting the power supply directly to ground. When the fire button is pushed, contact K15A (Figure D-11) in the trigger control circuit applies a pulse through tube EFP-60, pulse shaping transformer PE-5064-319 to the grid of a thyratron tube 5C22. The output of the thyratron is about 12 KV. The trigger is then passed through a 1:4 step-up transformer and applied through 1000 pf to the spark gap trigger circuit, causing the gap to break down. Gap breakdown allows the capacitor to discharge through the xenon flashtubes. Simultaneously, contact K9A opens and K8A closes. At this point the firing cycle is complete and the dump light on the local indicator panel should be lit. A portable fire button feature is installed to allow the experimenter to position himself in any desired location. For safety, the bank automatically assumes

a dump status for the following conditions: 1) immediately after firing, 2) if there is a misfire, 3) if there is a power failure, 4) if the system is purposely dumped. In the event that K8 failed in the open position, the capacitor would have to be discharged manually. Presently, when the system is in a dump status, the capacitor bank is connected to ground through a 9 megohm resistor and contacts K8A. In a misfire condition, the discharge time is $\sim$ 65 seconds. An improvement to the system would be to place the contacts of K8A in series with a much smaller resistor ($\sim$ 100K ohms) on the load side of the 9 megohm resistor, thus providing a nearly direct path to ground for the charge on the capacitor. A manual disconnect should be added to the grounding circuit to allow discharge of the capacitor in the event of failure of vacuum relay K8 in the open position. Figure D-5 shows the suggested alteration to the dump circuit which would allow faster discharge ($\sim$ 150 ms) of the capacitor than is presently available.

1. Capacitor, Wiring, Flashtubes and Reflector

Figure D-6 is a picture of the capacitor bank and shows the location of the four element spark gap. The capacitor is a low inductance 1.5 μf AXEL capacitor rated at 25 KV. It is set on a moveable metal cart. The cart and the steel capacitor case are maintained at ground potential. This arrangement facilitates moving the heavy capacitor around. Sheets of steel mesh of 70 mil thickness and 1/4 inch thick plexiglass surround the capacitor cart to protect laboratory personnel from a possible capacitor explosion and high

voltage arcing. A voltmeter, which has been modified by adding a 150 megohm resistance in series measures the voltage to which the capacitor is charged.

The capacitor is charged through shielded RG-8U high voltage cable. The RC time constant for a 1.5 μf capacitor in series with 9 megohm is about 13 seconds with a peak current of about 2.2 ma. (Total charge time is ∿ 5 time constants or ∿ 65 sec). The capacitor is discharged through a pressurized 4-element spark gap by command trigger from the control circuit via heavy gauge copper conductors, and then through the flashtubes to ground via braided copper high-current-capacity cable. All low current carrying circuits are wired with 12 gauge copper wire rated at 600 volts.

The flashtubes were donated by Sandia Labs for destructive testing. They are quartz tubes, 1.27 cm (1/2 in.) in diameter, 57.15 cm (22-1/2 in.) in length, and have a wall thickness of 1 mm (.0394 in.). They are fitted with COVAR end caps containing tungsten electrodes. The tungsten electrodes provide an arc length of 45.68 cm (18 in.). One end cap in each flashtube is drilled and fitted with a 1/8 inch diameter tube extension to allow gas filling. The tubes are filled with MATHESON Xenon (CP grade of 99.9% purity) to an initial pressure of 30 torr. The fill pressure can be varied and monitored for experimentation purposes via the small valves installed on the tubes and using the auxiliary xenon fill system incorporated in the laser system. The flashtubes are mounted parallel to the axis of the laser tube at a

voltage arcing. A voltmeter, which has been modified by adding a 150 megohm resistance in series measures the voltage to which the capacitor is charged.

The capacitor is charged through shielded RG-8U high voltage cable. The RC time constant for a 1.5 μf capacitor in series with 9 megohm is about 13 seconds with a peak current of about 2.2 ma. (Total charge time is ∿ 5 time constants or ∿ 65 sec). The capacitor is discharged through a pressurized 4-element spark gap by command trigger from the control circuit via heavy gauge copper conductors, and then through the flashtubes to ground via braided copper high-current-capacity cable. All low current carrying circuits are wired with 12 gauge copper wire rated at 600 volts.

The flashtubes were donated by Sandia Labs for destructive testing. They are quartz tubes, 1.27 cm (1/2 in.) in diameter, 57.15 cm (22-1/2 in.) in length, and have a wall thickness of 1 mm (.0394 in.). They are fitted with COVAR end caps containing tungsten electrodes. The tungsten electrodes provide an arc length of 45.68 cm (18 in.). One end cap in each flashtube is drilled and fitted with a 1/8 inch diameter tube extension to allow gas filling. The tubes are filled with MATHESON Xenon (CP grade of 99.9% purity) to an initial pressure of 30 torr. The fill pressure can be varied and monitored for experimentation purposes via the small valves installed on the tubes and using the auxiliary xenon fill system incorporated in the laser system. The flashtubes are mounted parallel to the axis of the laser tube at a

voltage arcing. A voltmeter, which has been modified by adding a 150 megohm resistance in series measures the voltage to which the capacitor is charged.

The capacitor is charged through shielded RG-8U high voltage cable. The RC time constant for a 1.5 μf capacitor in series with 9 megohm is about 13 seconds with a peak current of about 2.2 ma. (Total charge time is ∿ 5 time constants or ∿ 65 sec). The capacitor is discharged through a pressurized 4-element spark gap by command trigger from the control circuit via heavy gauge copper conductors, and then through the flashtubes to ground via braided copper high-current-capacity cable. All low current carrying circuits are wired with 12 gauge copper wire rated at 600 volts.

The flashtubes were donated by Sandia Labs for destructive testing. They are quartz tubes, 1.27 cm (1/2 in.) in diameter, 57.15 cm (22-1/2 in.) in length, and have a wall thickness of 1 mm (.0394 in.). They are fitted with COVAR end caps containing tungsten electrodes. The tungsten electrodes provide an arc length of 45.68 cm (18 in.). One end cap in each flashtube is drilled and fitted with a 1/8 inch diameter tube extension to allow gas filling. The tubes are filled with MATHESON Xenon (CP grade of 99.9% purity) to an initial pressure of 30 torr. The fill pressure can be varied and monitored for experimentation purposes via the small valves installed on the tubes and using the auxiliary xenon fill system incorporated in the laser system. The flashtubes are mounted parallel to the axis of the laser tube at a

radial distance of 5.08 cm (2 in.). They are mounted at this distance to allow longitudinal adjustment of the lengths of the laser which is between them. Figure D-7 shows the arrangement. The flashtubes are discharged in parallel to reduce magnetic field effects in the laser tube. An ionizing prepulse is applied to the flashtubes via jumpers which tap the main trigger pulse voltage and apply it directly to coils wrapped around the flashtubes. Nanoseconds later the main current pulse from the spark gap passes through the preionized flashtube, exciting the xenon gas.

The reflector is a double-confocal-elliptical cylinder 26.035 cm (10-1/4 in.) in length, with the laser tube at the common focus. The flashtubes are centered at the outer foci of the two elliptical cylinders. The internal surface of the reflector is highly polished to reflect a maximum amount of light at the wavelength $\lambda \simeq 280$ nm. Aluminum has a reflectance value of about 95% at that wavelength. Figure D-8 shows the overall dimensions of the reflector.

2. Spark Gap and Triggering System

The four element pressurized spark gap is identical to those described by Budzik [30], and was fabricated from component parts in stock at the laser-plasma laboratory at NPS. The switch is pressurized to allow reduction in gap size and therefore a low switch inductance. Pressurization of the switch makes possible easy adjustment of the standoff voltage. The use of the four element spark gap keeps jitter time and time for gas breakdown to a minimum [30]. The elements of

the gap are cylindrical to allow a large cross-sectional area and thus a very large current carrying capacity for the switch. Figure D-9 shows the arrangement of the four spark gap elements. Figure D-10 shows the electrical schematic of the gaps. The elements of the main gap are aluminum which has a low work function. The secondary trigger elements are tungsten pins which oppose each other across a small gap in the axial center of a stainless steel shield. The trigger element shield is placed so that it is out of the arc in the main gap. When the trigger is applied to the small gap, an electric arc produces ultraviolet light which ionizes the atmosphere in the vicinity of the main gap electrodes. When breakdown in the main gap occurs, current flows to the flashtubes.

The pressure vessel for the spark gap is made of one-inch thick plexiglass, bonded to itself with ethylene dichloride. Bolts provide extra strength. The pressure vessels have been tested to a pressure of 100 psi [30].

Nitrogen gas is used as an atmosphere in the spark gap. A low velocity flow of the gas through the spark gap insures purity of the atmosphere within the gap. The flow of the gas can be adjusted to provide a constant atmospheric pressure in the gap of 10 psi.

The trigger system is identical to that which is described by Budzik [30]. The system consists of a 10 KV thyratron pulse generator of 10 nanosecond duration, a 1:4 pulse transformer, and a spark gap. Figure D-3 is the electrical schematic of the trigger circuit.

D. OPTICAL CAVITY

The optical cavity of the oscillator is a hemi-confocal resonator. It consists of a spherical 98% reflector of 1.52 m (59.88 in.) radius (F1=760 mm) positioned about 86.4 cm (34 in.) from a 75% reflecting planar mirror at the other end. The spherical mirror was purchased from EDMUND SCIENTIFIC CORP. An opaque gold coating ($\sim$ 3000 Å thick) and a $\lambda/66$ thick SiO protective coating ($\sim$ 200 Å thick) are vacuum deposited on a substrate of glass for a reflectance of about 98% at the iodine laser wavelength (λ = 1.315 μm). The 1 inch (2.54 cm) diameter flat output window is 10 mm thick quartz on which a 110 Å thick gold coating and a 200 Å thick SiO protective coating has been vacuum deposited. The output window has a reflectance of about 75%. Included in the laser cavity are the active laser medium C_3F_7I, and an adjustable diaphragm (0.6 mm to 8 mm opening).

The hemi-confocal resonant cavity is similar to a hemispherical cavity except that its output planar mirror is positioned at the focal point of the spherical mirror instead of at the center of curvature. Some of the good features of the hemispherical cavity, listed by Bloom [31], apply to the hemi-confocal cavity. These include: 1) ease of alignment: Once the planar mirror is positioned perpendicular to and centered on the laser axis, further fine alignment can be accomplished using the spherical mirror; 2) use of the hemispherical cavity when lowest order mode operation is desired: By adjusting cavity length to slightly less than

the focal length (in our case Fl = 760 mm) and by proper use of a diaphragm, TEM_{oo} mode can be made certain [32]. (See the additional comments on alignment in Appendix G.)

The chief design consideration of the resonant cavity is its stability. Yariv offers [33], as do many other authors, simple calculations to test the stability of an optical cavity. The stability condition for an optical resonator is given by

$$S = 0 \leq (1 - \frac{L}{d_1})(1 - \frac{L}{d_2}) \leq 1 \qquad (3\text{-}1)$$

where L is the cavity length

d_1 and d_2 are the radii of mirrors #1 and #2, respectively.

Assigning values L = 86.4 cm, d_1 = 150 cm, $d_2 = \infty$, the stability of the resonant cavity may be calculated to be S = .424 which indicates a nicely stable confocal resonator.

IV. SUMMARY OF PRESENT STATUS OF THE IODINE LASER

The laser has been filled with 50 torr C_3F_7I, and $\sim$ 500 torr argon on numerous occasions and test fired approximately 200 times. Up to now there has been no indication that lasing has occurred. Presently, the maximum energy input to the flashtubes has been 432 Joules (24 KV and 1.5 μf).

A rough analysis was done to determine if the energy input is sufficient, in the present component arrangement, to produce a threshold population inversion for lasing. Gross estimates of coupling efficiencies (< 10%) and energy conversion efficiencies (1% in pump band for Xe and 60% C_3F_7I-Ar) were made. Calculations showed that possibly there is insufficient pumping energy being coupled into the laser tube to produce the necessary inversion for lasing. It is recommended that a more thorough analysis of this nature be conducted prior to making any changes to present laser configuration.

Some of the major problems that have impeded progress in building the laser-oscillator are: (1) The noise generated by the mechanical relay connections in the trigger circuit prevent close measurement of the trigger signal and flash-pulse characteristics, (2) Unavailability of proper detectors preclude measurements of pulse shapes for flash and laser output, (3) The use of flashlamps which are too long have prevented efficient use of pumping energy, (4) The present methods of monitoring pressure in the laser gas system requires

calibration prior to each use. The location of the installed variable-reluctance pressure gauge is such that there is no way to measure true pressure in the laser cell, (5) The present oscillator is mounted on a short rail which is secured to a tabletop. The present mount is subject to vibrations when the table is bumped. Thus, proper alignment is impossible.

There are four major problems which should be solved as soon as possible. They are: (1) Rid the trigger generator of the r-f noise caused by the relay switching, (2) Increase the efficiency of coupling input energy into the laser cell. This can be accomplished by:

(a) shortening the length of the flashlamps to make them more suitable to the laser tube length. Shorter flashlamps could be located closer to the laser cell to improve coupling of light energy into the laser gas;

(b) using a helical flashlamp to improve the coupling of light into the laser cell;

(c) increasing the number of linear flashlamps

(d) providing more energy into the flashlamps by increasing the capacitance of the capacitor bank which stores the pumping energy;

(3) Find a more positive method to monitor the laser gas pressure, (4) Purchase proper detectors to permit monitoring of both the pumping pulse and the laser output pulse.

The difficulties with alignment can be tolerated for the present time. However, after the laser begins operating, a more accurate alignment method must be devised.

APPENDIX A

CALIBRATION OF THE VARIABLE RELUCTANCE TRANSDUCER

The corrosive nature of C_3F_7I vapor dictates the use of materials which are corrosion resistant. The variable reluctance sensor permits measurement of absolute pressure of C_3F_7I while maintaining isolation of the pressure sensing device from the corrosive iodine vapor. A stainless steel diaphragm separates the sensor from the vapor. The difference in pressure on each side of the diaphragm is translated into a displacement of the diaphragm. The displacement is sensed as a reluctance change in the transducer's magnetic circuit. A resulting alteration of the circuit's self-inductance produces an emf which, after amplification, is measurable by a voltmeter.

To calibrate the variable reluctance pressure gauge, proceed as follows: Open valves 1, 3, 7 and 8 (Figure D-1), and pump laser gas system down to base pressure of 10^{-5} torr. All other valves are closed. For calibration purposes, 10^{-5} torr is considered zero system pressure. When the gas system is in this condition, adjust the sensor screw (Figure D-13) until about 1 volt full scale deflection can be read with no pressure in the system. Fine adjustment can be made with the screw on the sensor amplifier. Be sure the voltmeter has been properly zeroed. Close valves 1 and 3 to isolate the vacuum system. Open the argon bottle and set the regulator for

about 16 psi. Open valve 9 slowly and watch the pressure gauge behind valve 4. Let it build to about one atmosphere (760 torr). Valve 4 now can be used to slowly "bleed" argon into the transducer. By comparing the numerical reading on the pressure gauge to the voltage readout, the reluctance pressure sensor can be calibrated. Take an average of a number of sets of readings and plot the curves. The calibration curve is shown as Figure A-1.

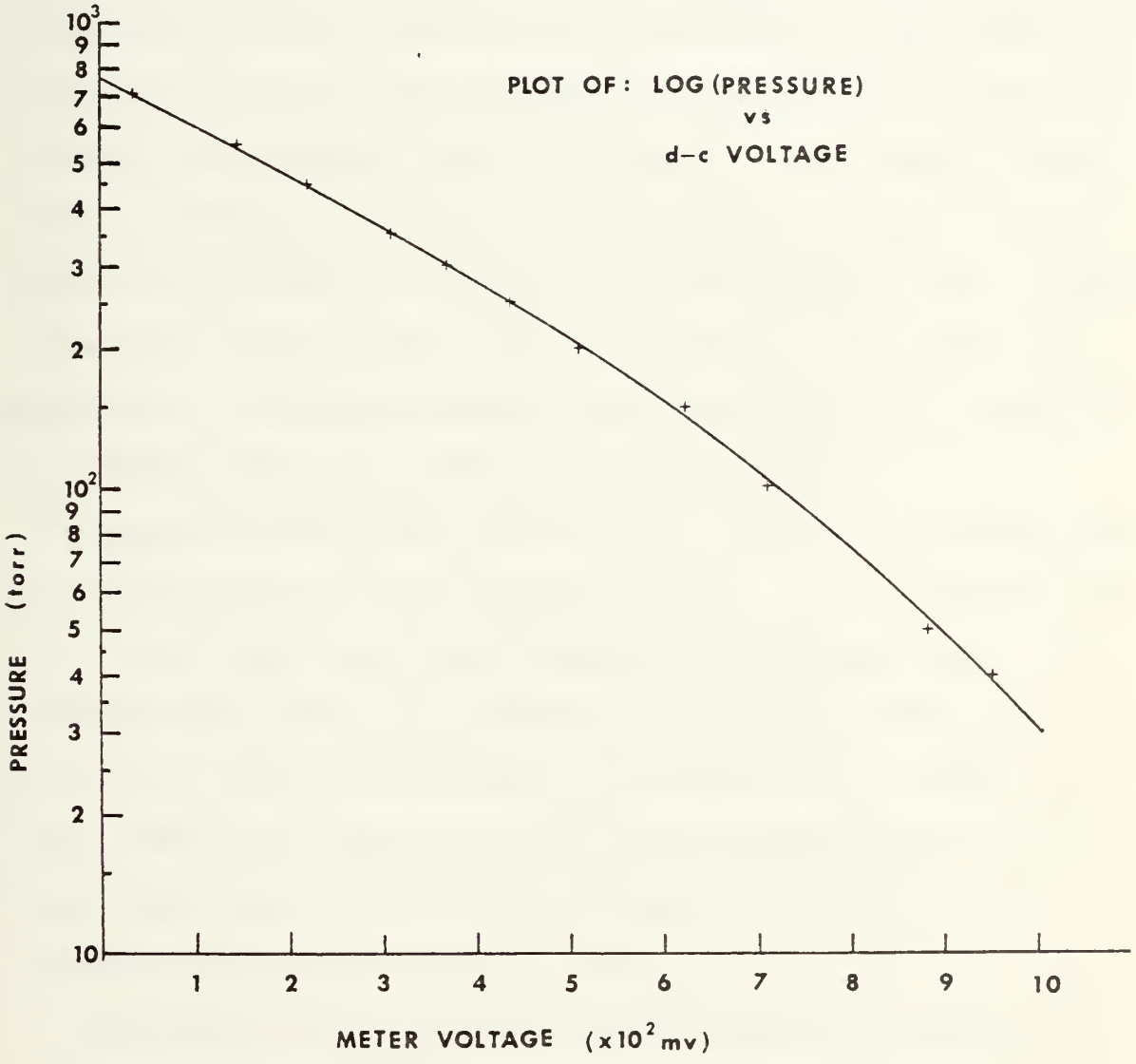

FIGURE A-1 Calibration Curve for Variable Reluctance Transducer

APPENDIX B

LASER GAS FILLING/DUMPING PROCEDURE

Filling procedure for the oscillator is as follows: The system is pumped down to a base pressure of $\sim 10^{-5}$ torr with valves 7 and 8 open. Valve 3 is open to allow zero setting of the variable reluctance pressure transducer. After setting transducer at zero, close valve 1 and slowly "crack-open" the valves 5 or 6 on the tank containing the distilled C_3F_7I and let the vapor diffuse into the system to a desired pressure up to a maximum of 125 torr. Then close the tank valve and allow the pressure in the system to reach equilibrium. Valves 7 and 8 are then closed. The oscillator is now ready for operation. Continuous monitoring of oscillator pressure can be accomplished with valves 7 or 8 and 3 open.

Dumping of the master oscillator contents is accomplished by opening valve 1 to the vacuum system. It is important not to let the iodine vapor go through the diffusion pump. The forepump only should be employed. During this evolution, valves 2, 5, and 6 are closed and valves 1, 3, 7, and 8 are open. When the inlet pressure of the vacuum system reaches about 3 microns, it is safe to engage the diffusion pump to complete the pump-down to 10^{-5} torr.

Provision has been made for investigation of pressure broadening effects of rare gases on the lasing medium. An injection source using MATHESON argon of 99.998% purity is

included in the oscillator gas system. The valving network in the argon injection system permits filling of the laser to any desired partial pressure of argon.

Initial filling or replenishment of C_3F_7I is done as follows: Open valves 1, 3, 7, 8 and the valve (5 or 6) on the tank that does not contain C_3F_7I. Evacuate the system to base pressure (10^{-5} torr). After pumpdown, close valves 1, 7 and 8. (If tank connected to filler tube contains C_3F_7I, distill it over to the other tank and evacuate the fillertank. Close valve 6, leaving filler tank under vacuum. Prepare the bottle of C_3F_7I for transfer of contents. Remove filler cap of filler tube and insert a small funnel. Begin pouring C_3F_7I into the funnel. Simultaneously "crack" the filler valve. The vacuum in the tank will suck the C_3F_7I into the tank. Close the filler valve. The evolution is complete after distillation according to the procedure discussed in Appendix C.

APPENDIX C

LASER GAS PURIFICATION PROCEDURE

Each cycle of the purification process involves two stainless steel tanks, one containing C_3F_7I and one empty tank. Valves 5 and 6 are closed and the main gas system is evacuated to system base pressure ($\sim 10^{-5}$ torr), and then valves 1, 4, 7 and 8 are closed. Valve 3 is open to permit pressure measurement. The empty tank is cooled by a dewar containing a CO_2-methanol bath. The valves 5 and 6 of the two tanks are opened and the tank containing C_3F_7I is heated to 40° C (104° F). The C_3F_7I boils and recondenses in the cooled tank. The end of the distilling process is signaled by a drop in pressure. The cooled tank then contains the C_3F_7I and may be valved off from the system by closing valve 5 (or 6). Valve 1 may be opened to pump down residual CO_2 and O_2 and the original tank may be baked out to drive off any water vapor present. This process can be repeated until a purity is reached, which is sufficient for lasing action. Best laser action occurs when C_3F_7I vapor has a clear appearance. The vapor becomes pink when it contains I_2. When I_2 is present it quenches laser action prematurely. Therefore, the laser gas must be distilled enough to remove the pink hue. The color of the vapor can be observed by looking down the laser bore when the tube is filled.

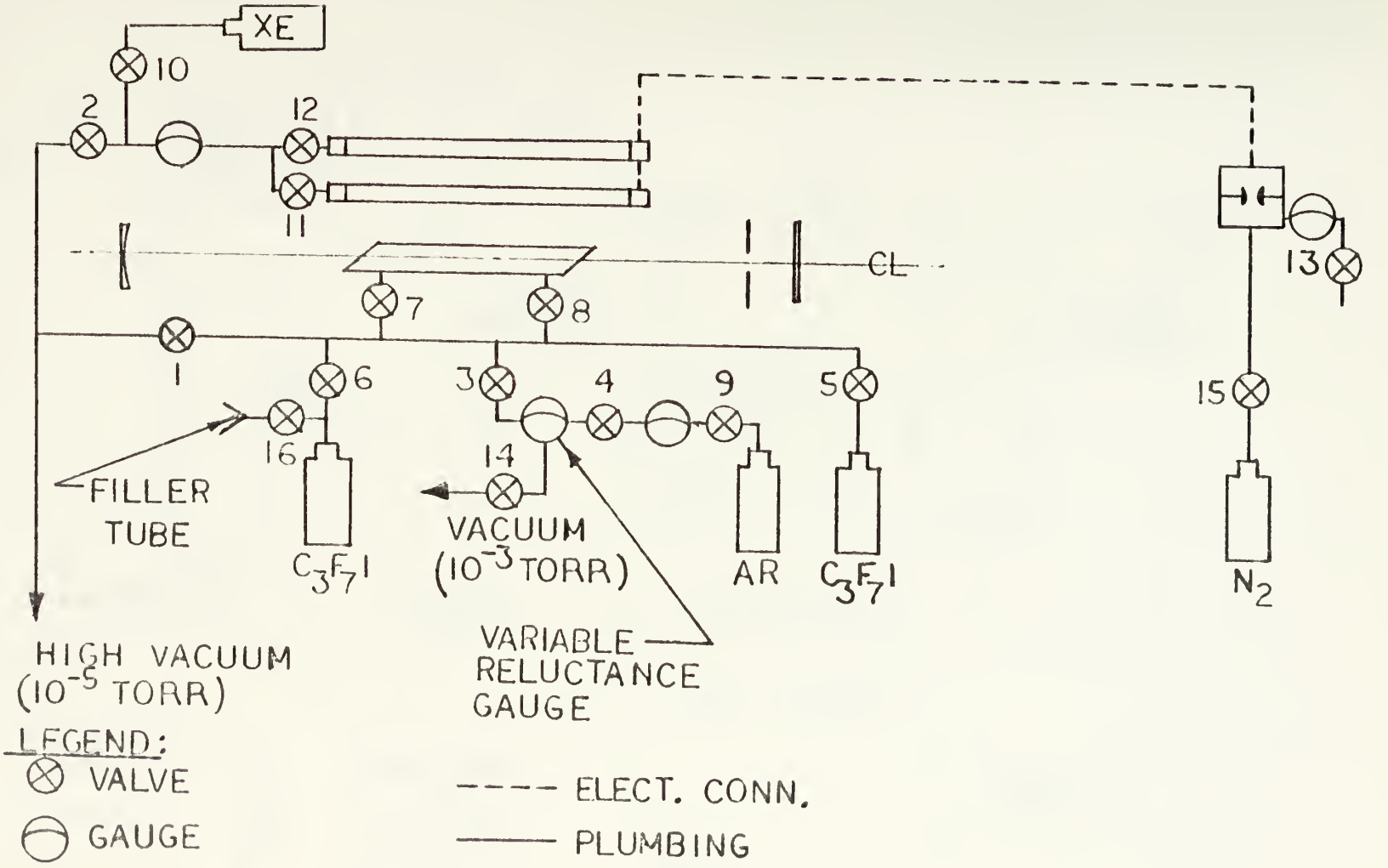

FIGURE D-1 VACUUM/GAS TRANS/PURIFICATION SYST.

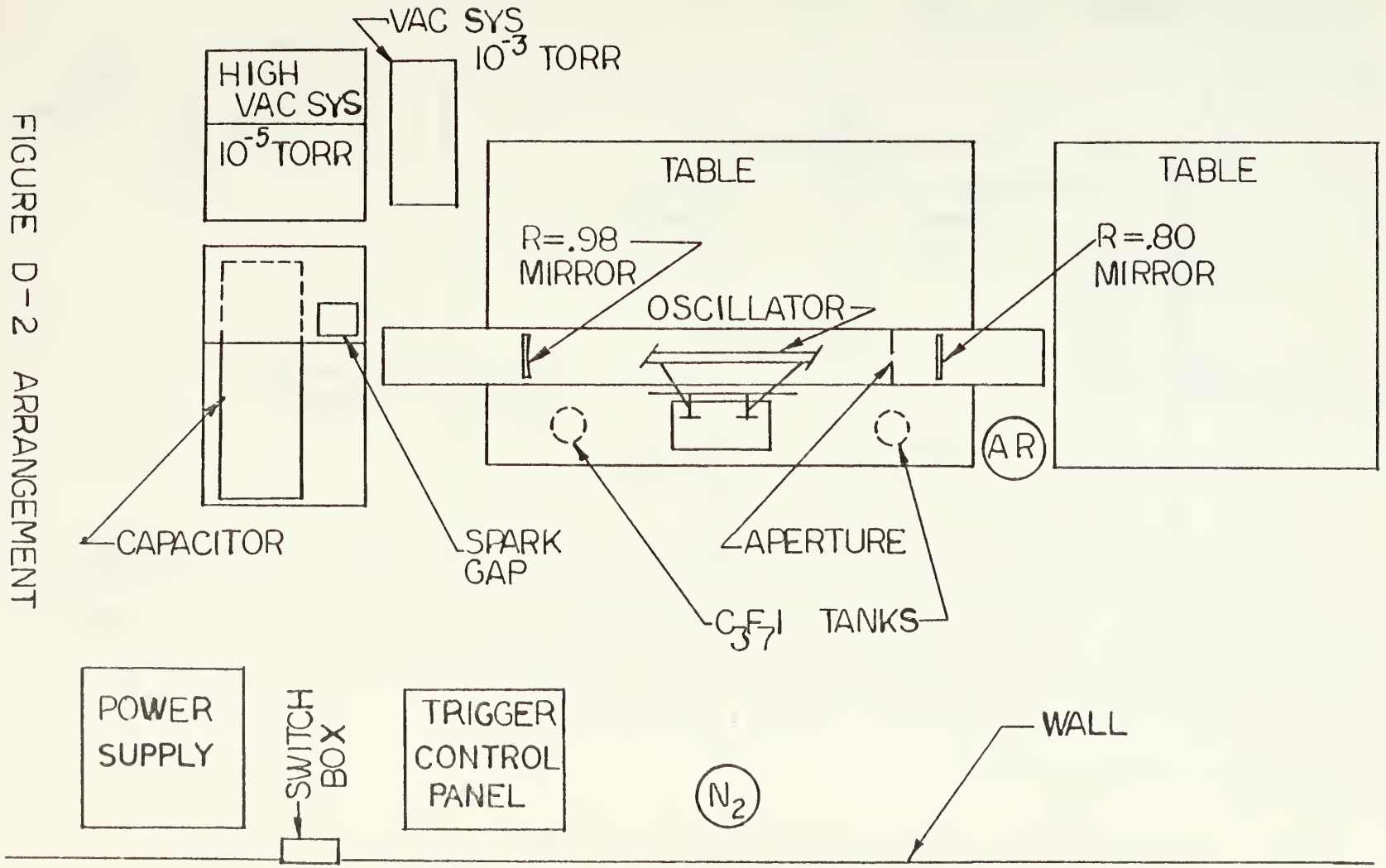

FIGURE D-2 ARRANGEMENT

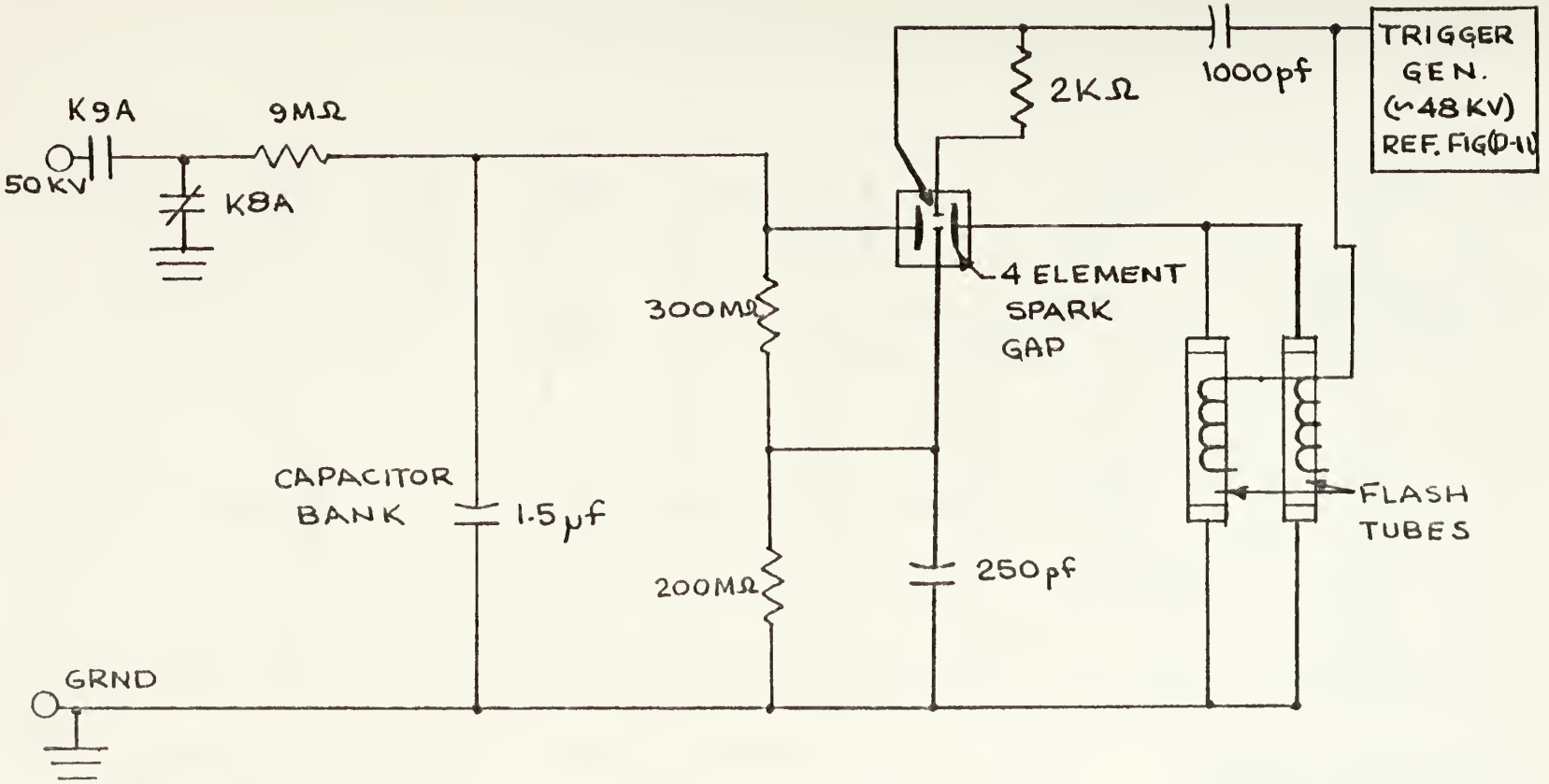

FIGURE D-3 CAPACITOR CHARGE/DISCHARGE AND TRIGGER CIRCUITS

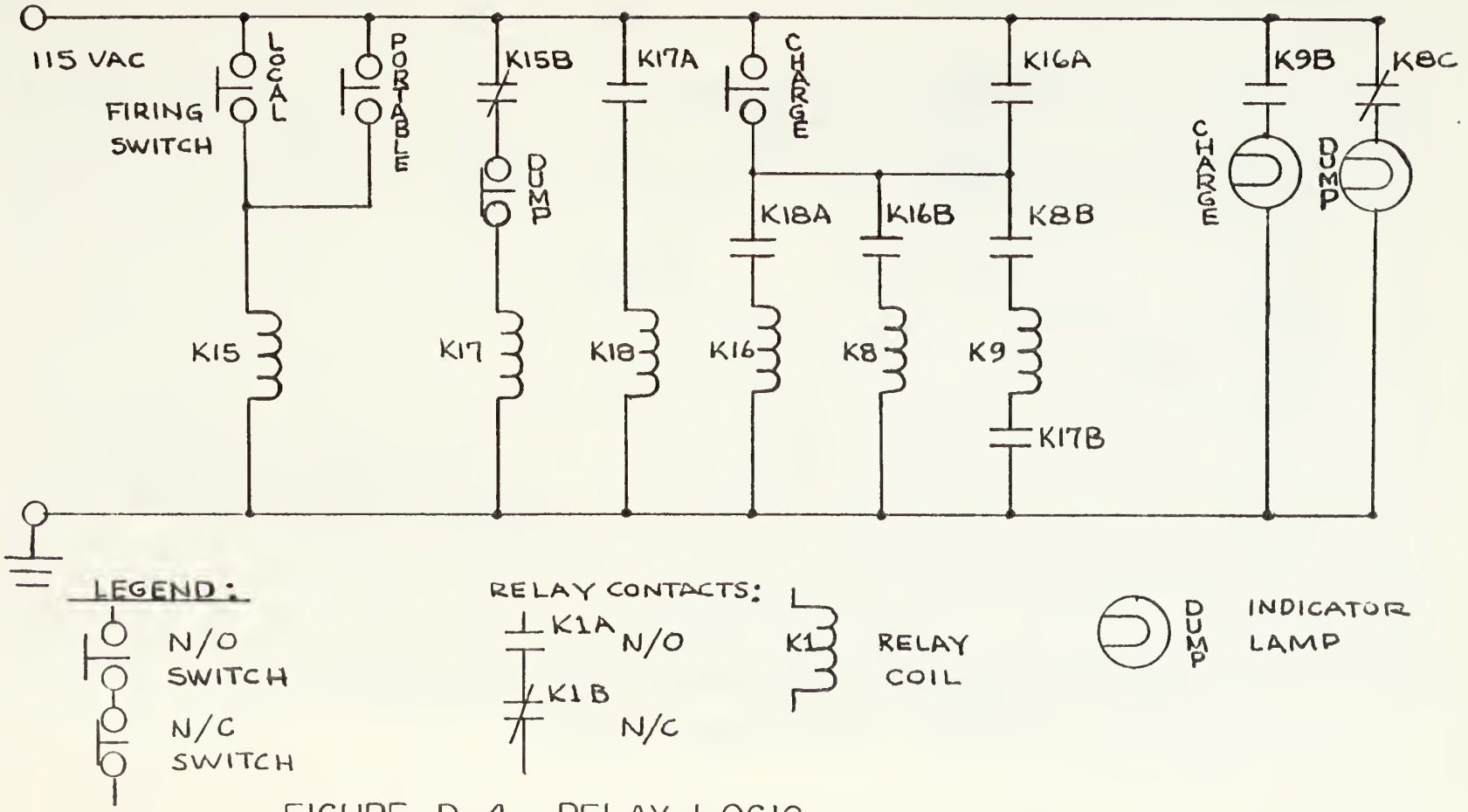

FIGURE D-4 RELAY LOGIC

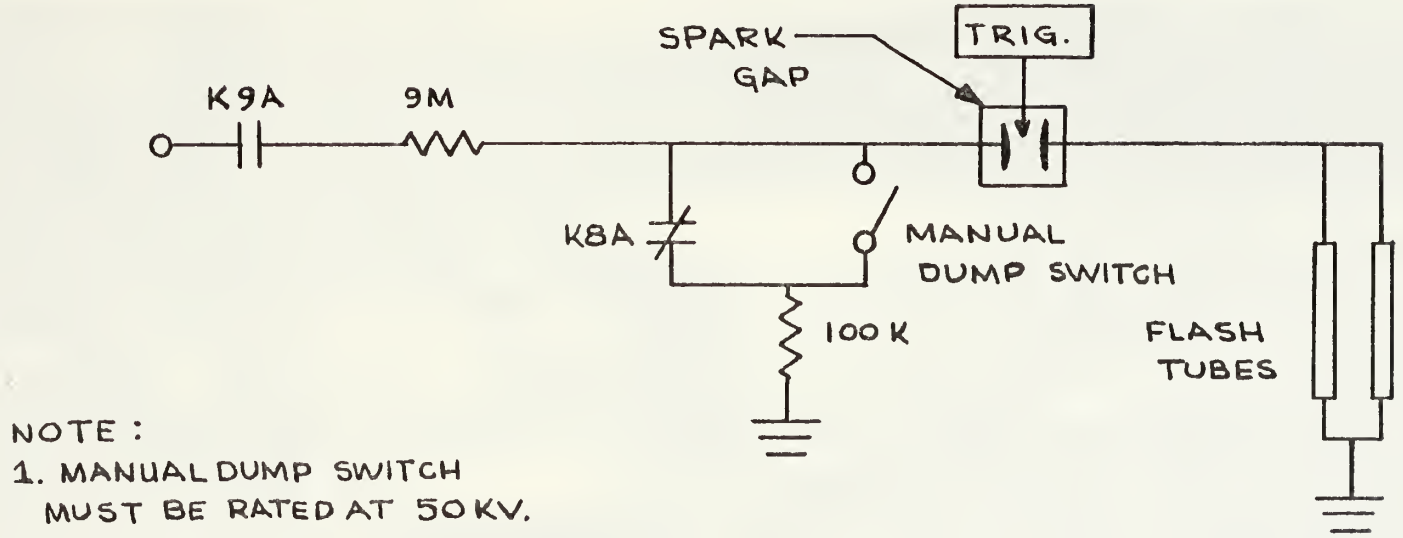

FIGURE D-5. PROPOSED ALTERATION TO 50 KV POWER SUPPLY DUMP CIRCUITS.

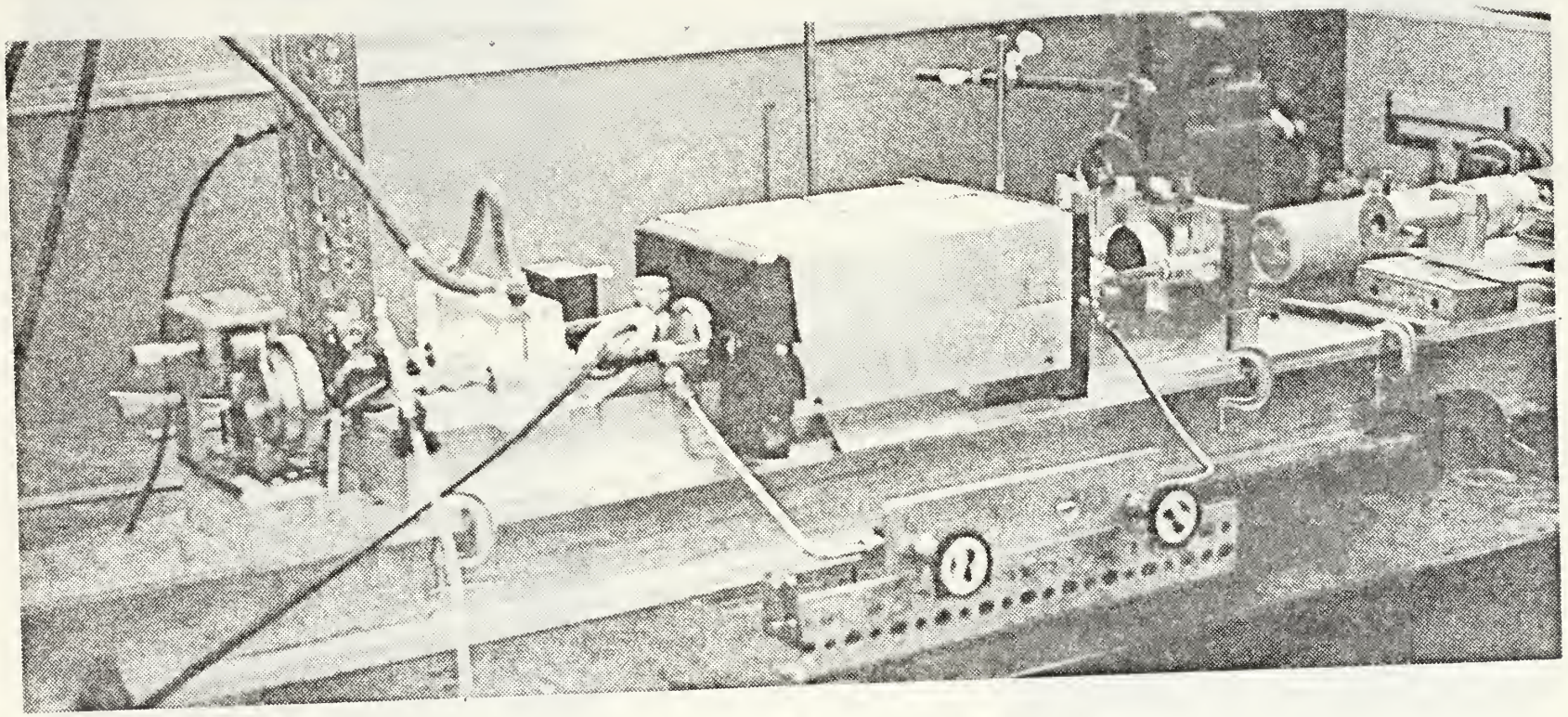

FIG. D-6a Iodine Laser-Oscillator

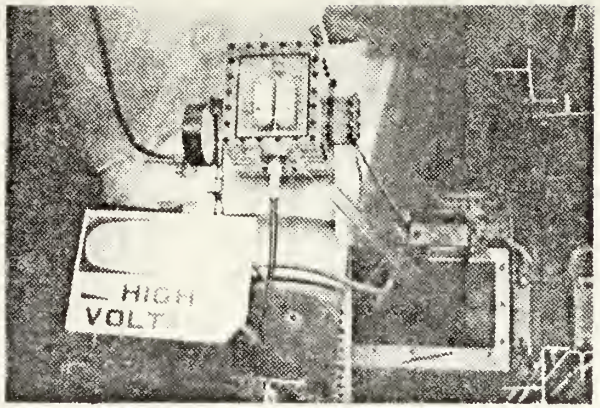

Spark Gap and Capacitor

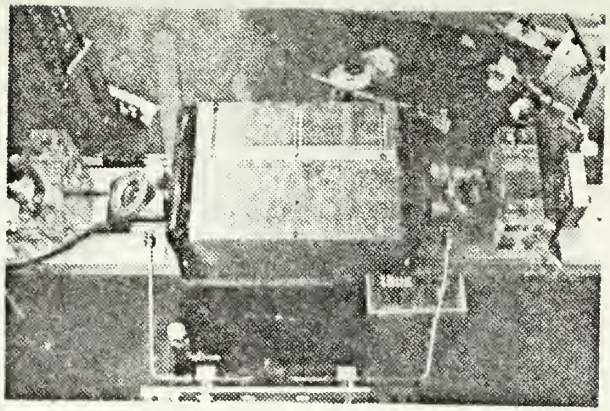

Laser Top View

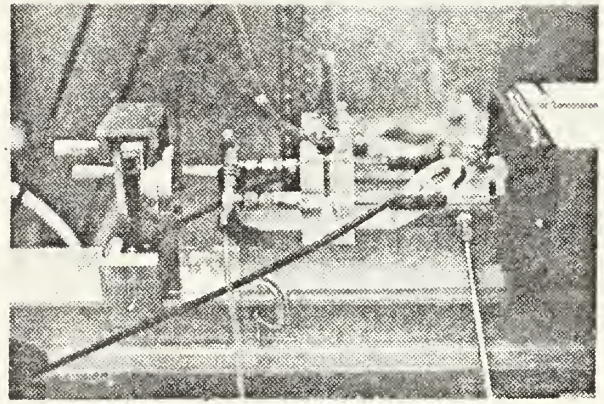

Laser Head and 97% Mirror

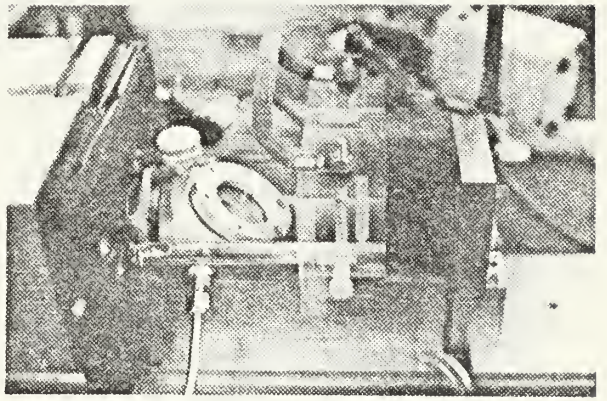

Laser Head and 75% Mirror

FIGURE D-6b

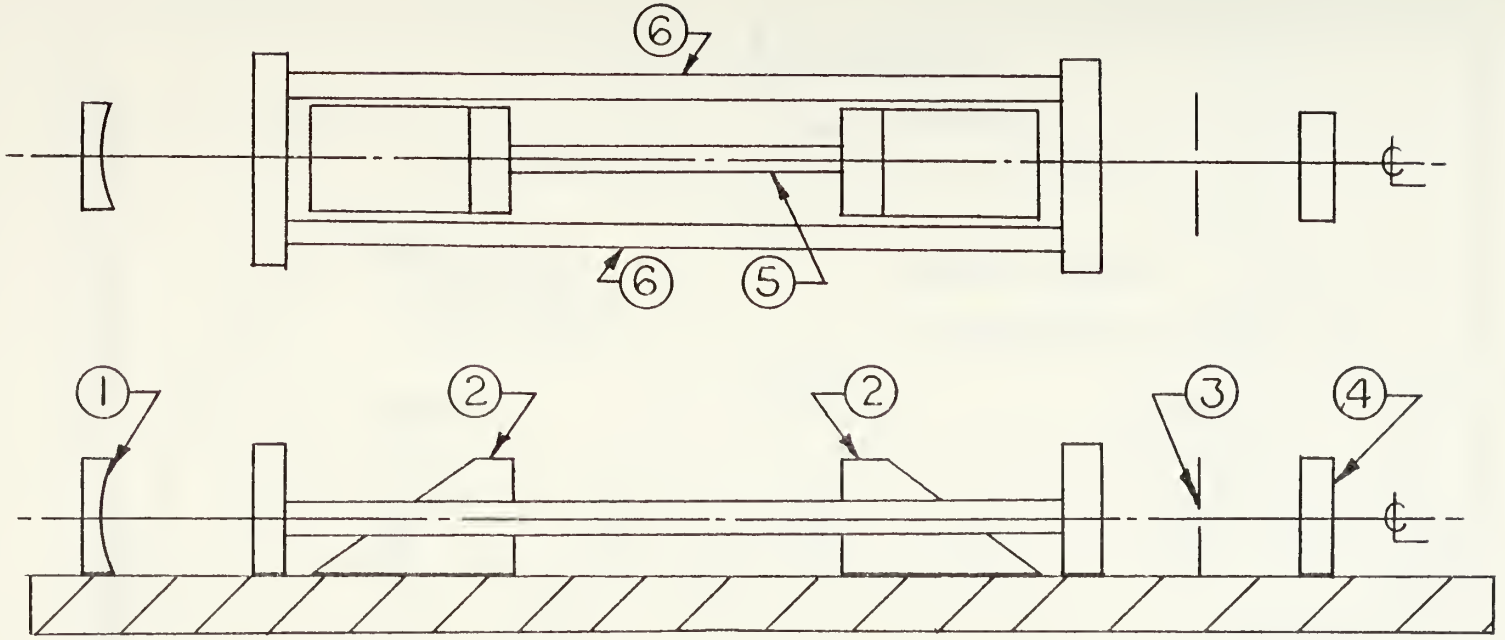

1 SPHERICAL MIRROR (R.=.98 , RAD.=1.5 M , F.L.=.75M)
2 MONEL LASER HEADS
3 APERTURE
4 FLAT OUTPUT MIRROR (R≈.80)
5 SUPRASIL LASER TUBE
6 QUARTZ FLASH TUBES

FIGURE D-7 ORIENTATION OF COMPONENTS

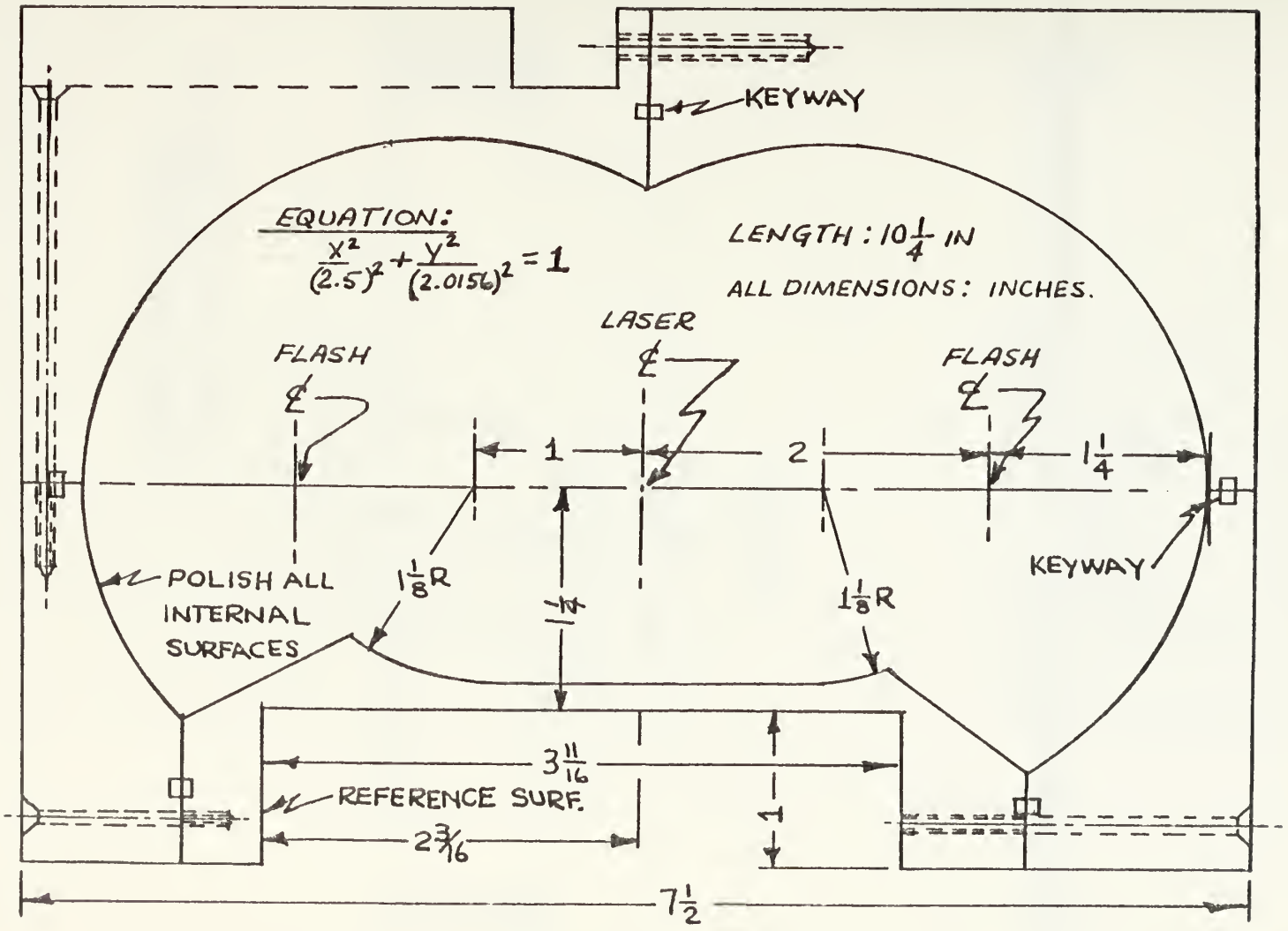

FIGURE D-8 DOUBLE-CONFOCAL-ELLIPTIC REFLECTOR

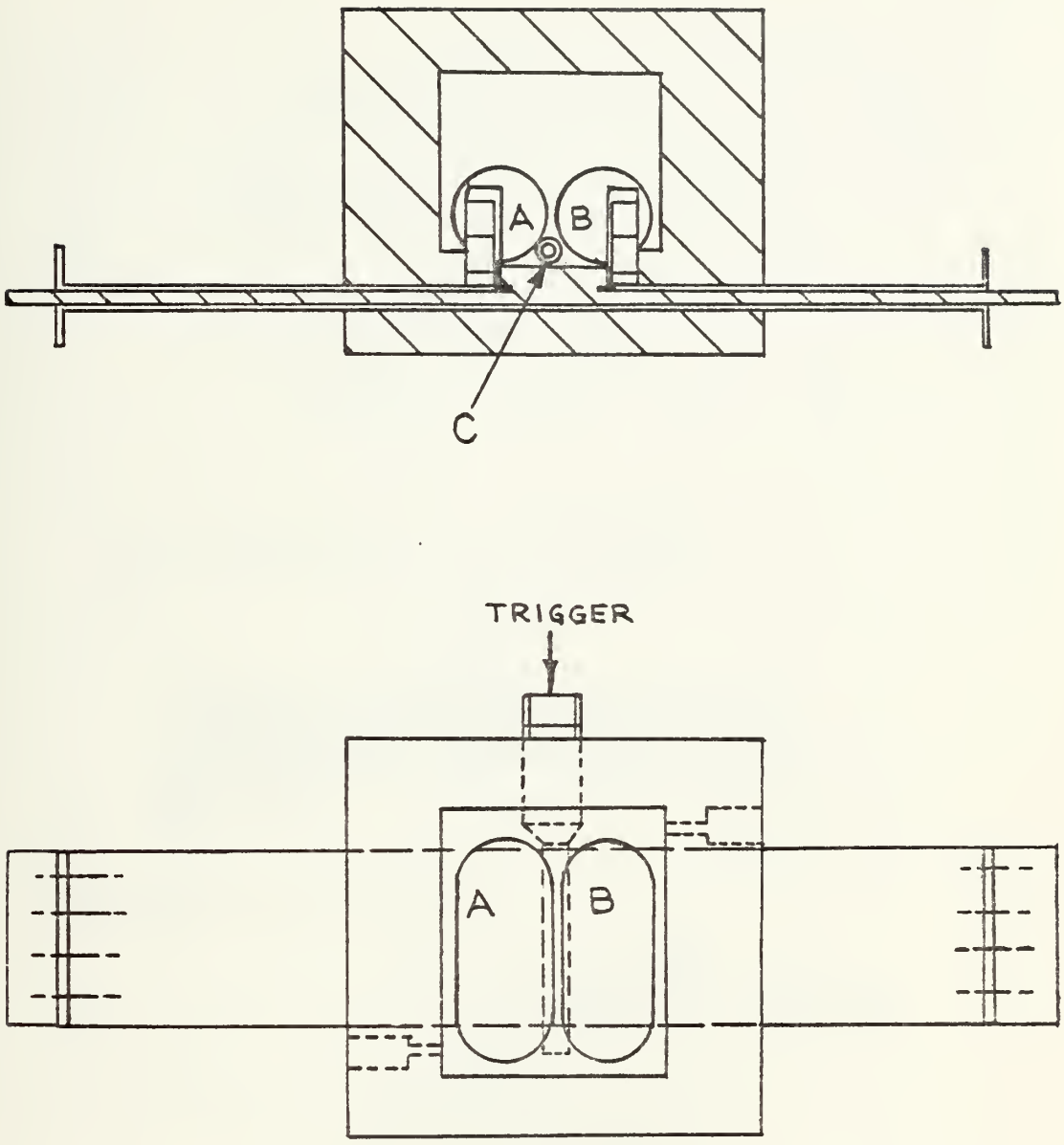

A,B MAIN ELECTRODES

C TRIGGER ELECTRODE

FIGURE D-9 SPARK GAP SCHEMATIC

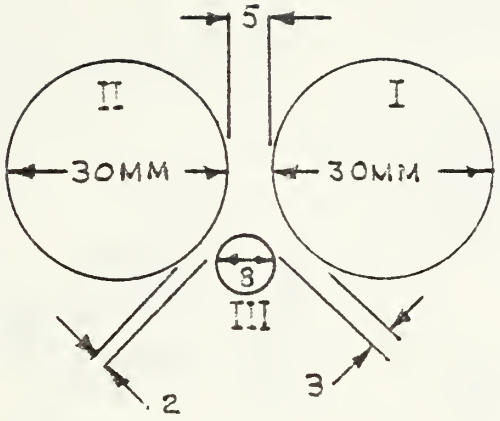

ALL DIMENSIONS IN MILLIMETERS

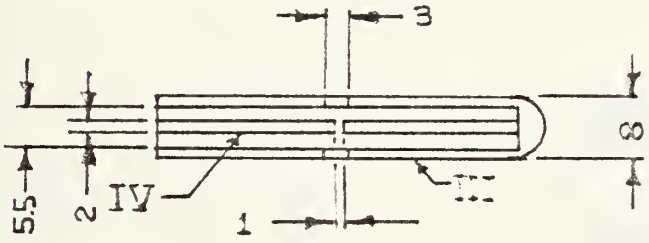

TRIGGER GAP GEOMETRY

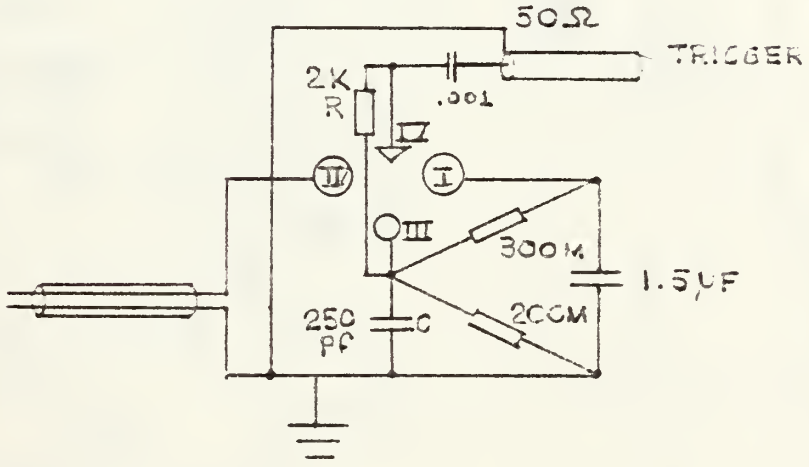

SPARK GAP CIRCUIT

FIGURE D-10

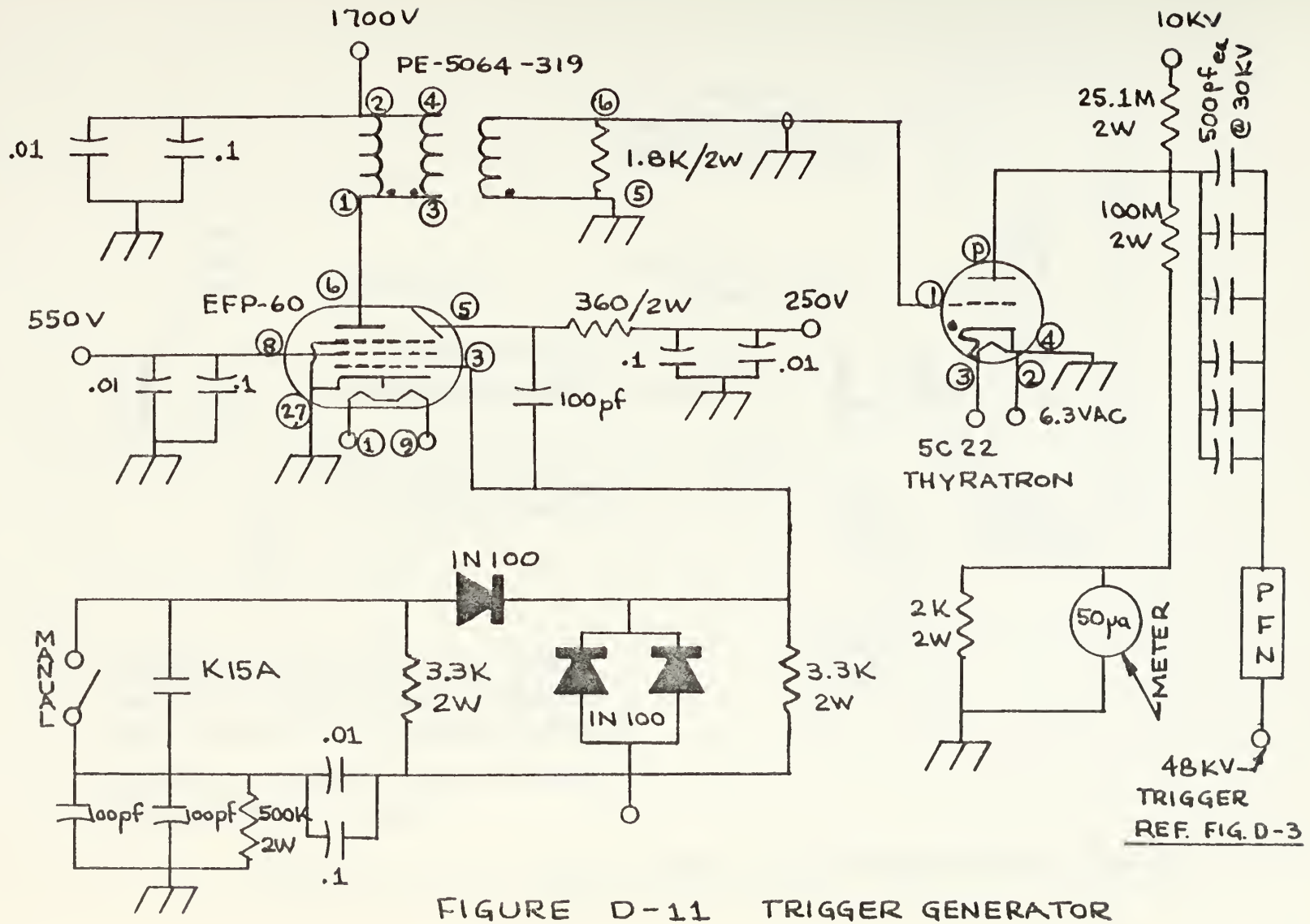

FIGURE D-11 TRIGGER GENERATOR

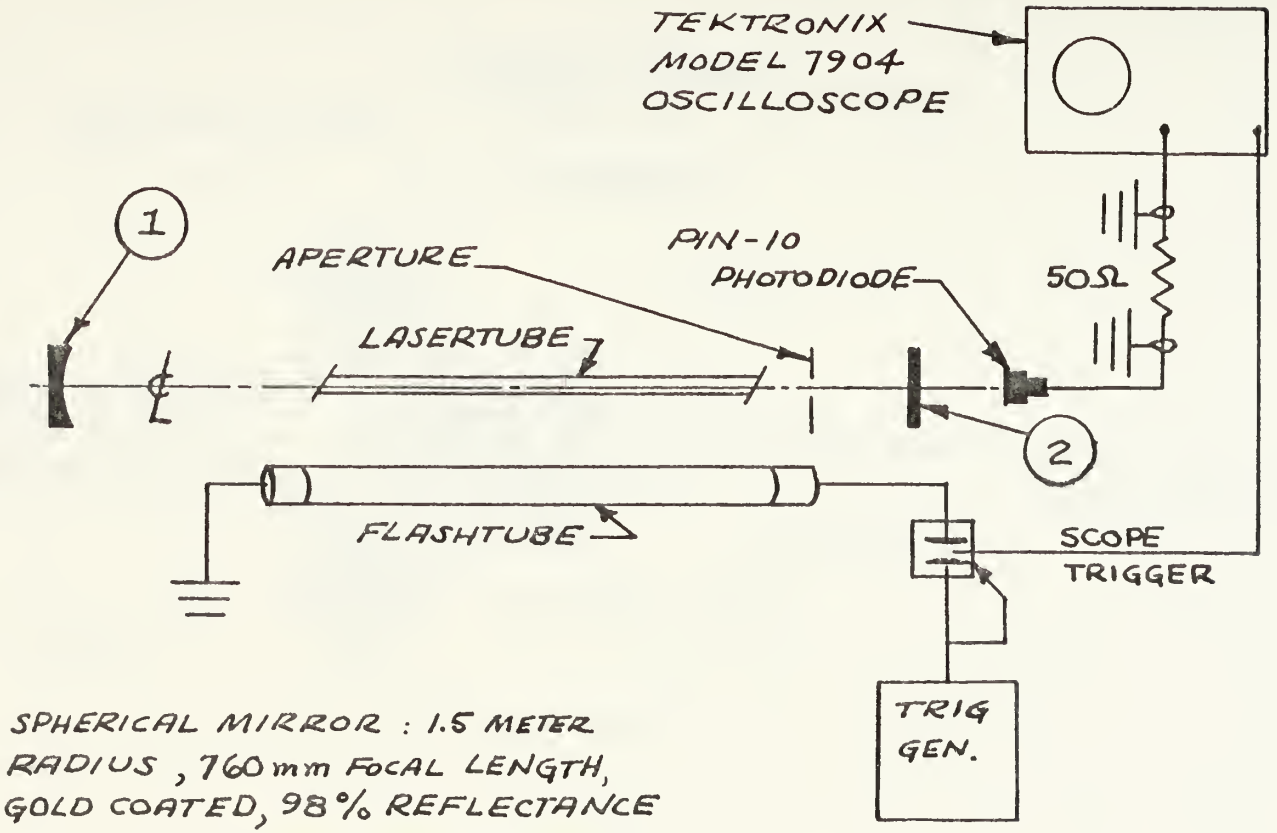

1. SPHERICAL MIRROR : 1.5 METER RADIUS , 760 mm FOCAL LENGTH, GOLD COATED, 98% REFLECTANCE
2. PLANAR MIRROR , GOLD COATED, 80 % REFLECTANCE.

FIGURE D-12 SCHEMATIC OF EXPERIMENTAL SETUP

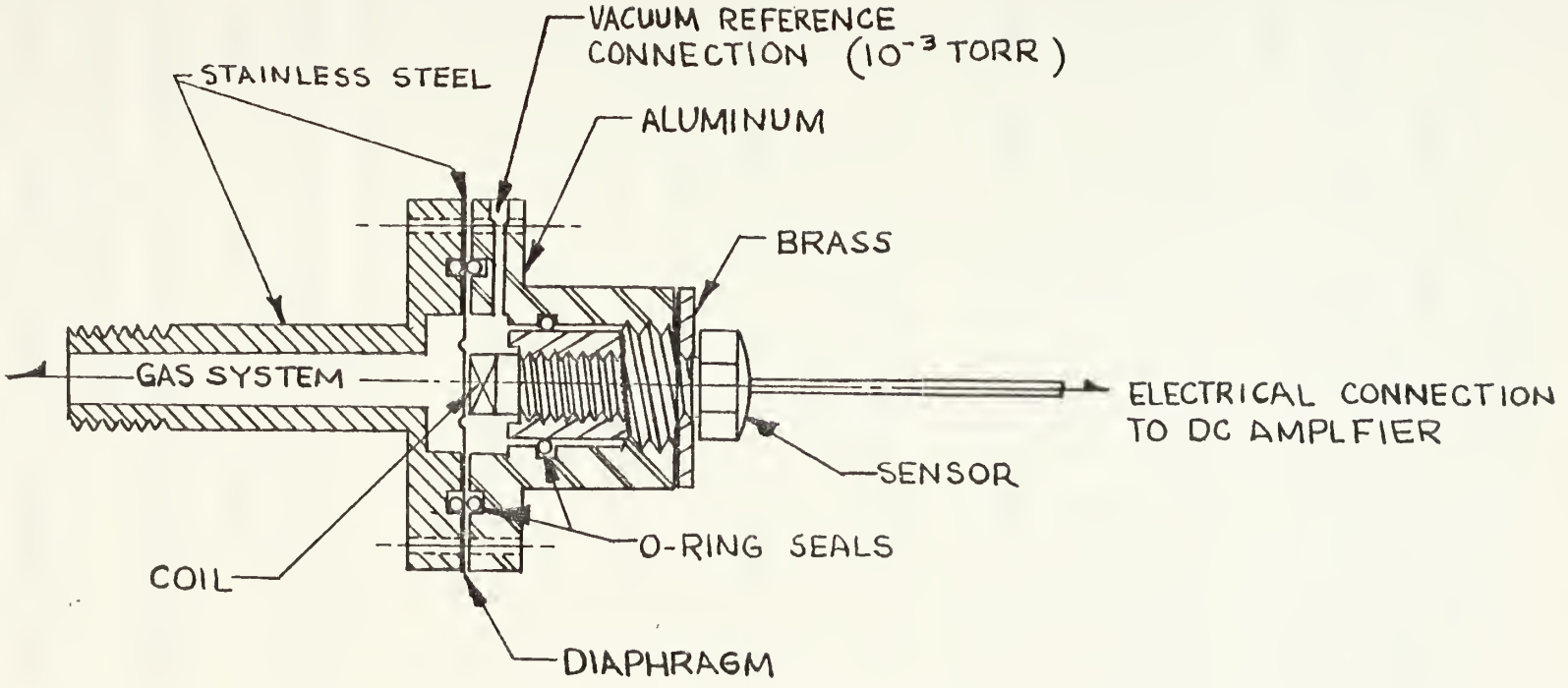

FIGURE D-13 VARIABLE RELUCTANCE PRESSURE GAUGE

APPENDIX E

POWER SYSTEM LIGHT-OFF/SHUT-DOWN

A. The procedure for energizing the high voltage power supply is as follows:

1. Switch breaker #10 in switch box on wall adjacent to the 50 KV power supply to ON position.
2. Switch to ON position the following switches on the lower panel of the 50 KV power supply door:
    a. fan
    b. rectifier filaments
    c. auxiliary power
3. Press START button and wait about two minutes for HV READY light to appear.
4. Switch ON the 50 KV ganged circuit breaker on lower panel of power supply door.
5. Adjust the meter-relay pointer to a safe maximum voltage.
6. Press the HV-ON button.
7. Adjust the HV CONTROL variac to desired output.

The power supply is ready for operation.

B. The procedure to secure the HV power supply follows:

1. Press the HV-OFF button.
2. Press the RESET button to complete the discharge of internal capacitors.
3. Switch OFF the filaments and 50 KV breaker

4. Switch OFF breaker #10 in wall switch panel.

C. The procedure to energize the trigger-control circuits is as follows:

1. Switch ON the power switch on the lower section of the control panel. This switch applies 115 VAC to all the relays and initiates a 1 minute timer.
2. When HV READY light appears on the lower panel, switch ON the switches marked HV-ON (lower panel) and FIL-ON (trigger generator panel) and await the appearance of the HV light on the trigger generator panel.
3. Adjust the variac on the lower panel until the 15 KV meter reads 12.5 KV.
4. Adjust the potentiometer knob on the trigger generator panel for a reading of $\sim$ 1.7-1.8 KV on the adjacent 2 KV meter.
5. The system is now ready to fire.

D. Securing the control panel is simply the reverse of part C.

APPENDIX F

PROCEDURE FOR FILLING THE FLASHTUBES WITH XENON

The procedure for filling the flashtubes with xenon gas is as follows: (reference to Figure D-1 is urged)

Initial fill:

1. Open valves, 2, 11, 12 and permit two hours or more for the tube pressure to reach system base pressure of 10^{-5} torr.
2. After reaching base pressure, close valve 2 to isolate flashtube gas system from vacuum system.
3. With valve 10 closed, open xenon bottle and adjust the regulator to about 1 psi (50 torr).
4. Open valve 10 and allow the tubes to fill (almost instantly).
5. When fill is complete, close tightly valve 10 and the valve on the xenon bottle.
6. Close valves 11 and 12.

The flashtubes have a volume of approximately 9.42 in. ($\sim$ 154.4 cm^3).

To change flashtube pressure, proceed as follows:

1. Purge the charged line by opening valve 2 while valves 10, 11 and 12 remain tightly closed. This removes air that may have leaked into the line.
2. To add: Close valve 2 and open xenon bottle, adjusting regulator to desired pressure. Open valve 10, 11, 12 and add xenon to desired pressure.

3. To decrease: Be sure valves 10, 11 and 12 are tightly closed. Open valve 2 and evacuate the filler line. Close valve 2 and open valve 11(12) until desired pressure registers on the gauge adjacent to valve number 2. Close number 11(12), evacuate the unwanted xenon and repeat the process with the other flashtube.

A cold trap should be added to the xenon line. This would enable recapturing this precious and expensive gas.

APPENDIX G

ALIGNMENT NOTES

The axis of the lowest order mode must lie along the line intersecting the center of curvature of the spherical mirror that is perpendicular to the flat mirror. Bloom [31] makes the following comments regarding the hemispherical resonator which also apply to the hemiconfocal arrangement:

> "....The motion of the spherical mirror does not swing the mode-spot on the flat mirror but instead displaces the entire mode while keeping the axis parallel. This can perhaps be seen by imagining a surface tangent to the spherical mirror that is parallel to the flat; it is then seen that displacing the sphere is equivalent to rolling the sphere on the flat. For this reason care must be taken in aligning a hemispherical resonator to be sure that the mode is accurately parallel to the axis of the laser bore before final alignment of the spherical mirror. The final touch-up on the sphere merely places the mode accurately in the center of the bore."

The foregoing points to the fact that the initial alignment of the flat mirror so that the laser bore axis and the beam are parallel (i.e., the mirror perpendicular to the axis) is critical to proper lasing.

APPENDIX H

FLASHPULSE/LASER ENERGY OUTPUT MEASUREMENTS

Actual measurement of flashpulse and laser output pulse characteristics has been plagued by difficulty. The laser is pumped in the ultraviolet region in a 500 Å bandwidth centered about 2680 Å. Lasing occurs at a wavelength of 1.315 μm. Both the pumping bandwidth and the laser output fall in a region of the electromagnetic spectrum which has not been studied at NPS. Therefore, the detectors required to make measurements on the pulse parameters of the xenon flash and the laser output are presently unavailable in NPS stock.

Flashpulse parameter measurement requires a filter to measure the output in a waveband 2680 ± 250 Å and a photo-emitting device (probably CsSb) with a time constant of $\sim$ 1 μsec. Laser pulse parameter measurement requires a photoconducting device (probably InSb or GeAu) with a time constant less than 1 μsec. The expected laser pulse is in the 1 to 10 nsec range.

Measurements of both the flashpulse and the laser pulse were attempted with some detectors, namely, a silicon p-i-n photodiode and a TROPEL Model 330 photodiode. The attempt proved futile. No attempt was made to filter out the light from the visible portion of the spectrum to check the detector's response in the region of interest.

In order to determine whether lasing does occur in the oscillator, two methods were employed:

1. An ELECTROPHYSICS CORP. Model 7100 INFRARED Viewer was used to sight down the laser bore during six of the firings. The flashtubes were covered to prevent the flash from blanking the viewer. During the flash a very intense radiation from the laser bore propagated down the axis and blanked the viewer screen.
2. Measurements of the energy propagating along the laser axis were attempted, using a HADRON Ballistic Thermopile Model 118 in conjunction with a KEITHLEY Model 149 Milli-microvoltmeter. This method revealed a pulse output from the laser-oscillator of 1-2 millijoules on 12 successive firings. This pulse was discovered to be r-f noise from the trigger system. The laser tube as filled with 50 torr C_3F_7I and 470 torr argon. The capacitor was charged to 20 KV for each firing and discharged on trigger command.

It is recommended that further characteristic measurements be made of both the xenon-pumping pulse and the laser output when the aforementioned proper detectors become available.

LIST OF REFERENCES

1. J. V. Kasper, C. G. Pimentel, "Atomic Iodine Photodissociation Laser," Applied Physics Letters, Vol. 5, No. 11, p. 231 (1964).

2. M. A. Pollack, "Pressure Dependence of the Iodine Photodissociation Laser Peak Output," Applied Physics Letters, Vol. 8, No. 2, p. 36 (1966)

3. Laboratories with current work in progress are:
Sandia Labs, Albuquerque, New Mexico, 87115
Lawrence Livermore Labs, Univ. of Cal, Livermore, CA 94550
Max-Planck-Institut fur Plasmaphysik, EURATOM Association, Garching, Germany
A. A. Zhdanov Leningrad State University, USSR
P.N. Lebedev Physics Institute, USSR Academy of Sciences USSR
Bell Telephone Laboratories, Holmdell, New Jersey, 07733

4. P. Gensel, K. Hohla, K. L. Kompa, "Energy Storage of CF_3I Photo Dissociation Laser," Applied Physics Letters, Vol. 18, No. 2, p. 48 (1971)

5. D. Porret, C. F. Goodeve, "Continuous Absorption Spectra of Alkyl Iodides and Alkyl Bromides and Their Quantal Interpretation," Proceedings of the Royal Society (London), A 165, 31, 1938.

6. J. V. Kasper, J. H. Parker, G. C. Pimentel, "Iodine-Atom Laser Emission in Alkyl Iodide Photolysis," Journal of Chemical Physics, 43, 1827 (1965)

7. V. Y. Zalesskii, A. A. Venediktov, "Mechanism of Generation at the $5^2P_{\frac{1}{2}} \rightarrow 5^2P_{\frac{3}{2}}$ Transition in Iodine," Soviet Physics JETP, 28, 1104 (1968)

8. V. Y. Zalesskii, E. I. Moskalev, "Optical Probing of a Photodissociation Laser," Soviet Physics-JETP, 30, 1019 (1970)

9. G. A. Skorobogatov, V. S. Komarov, and V. G. Seleznev, "Absolute-Photometry Determination of the Rate Constant of the Gas Phase Reaction of the Radical Compound C_3F_7 and I ($^2P_{3/2}$)" Soviet Physics Technical Physics, Vol. 19, No. 9, 1239 (1975)

10. V. S. Zeuv, V. A. Katulin, V. Y. Nosach, O. Y. Nosach, "Luminescence Spectrum of Atomic Iodine," Soviet Physics JETP, 35(9) 870 (1972)

11. R. G. Derwent, B. A. Thrush, "The Radiative Lifetime of the Metastable Iodine Atom $I(5^2P_{1/2})$," Chemical Physics Letters, 9, 591 (1971)

12. K. Hohla, "The Iodine Laser, A High Power Gas Laser," a Paper Presented at the Third Workshop on "Laser Interactions and Related Plasma Phenomena," at Rensselaer Polytechnic Institute, Hartford Graduate Center, August 13-17, 1973.

13. E. D. Jones, M. A. Palmer, F. R. Franklin, "Subnanosecond High Pressure Iodine Laser Oscillator," Preprint, submitted for publication.

14. K. Hohla, K. L. Kompa, "Gigawatt Photochemical Laser," Applied Physics Letters, 22, 77 (1973)

15. W. C. Hwang, J. V. Kasper, "Zeeman Effects in the Hyperfine Structure of Atomic Iodine Photo Dissociation Laser Emission," Chemical Physics Letters, 13, 511 (1972)

16. W. T. Silfvast, L. H. Szeto, O. R. Wood, "C_3F_7I Photo Dissociation Laser Initiated by a CO_2-Laser-Produced Plasma," Applied Physics Letters, 25, 593 (1974)

17. V. S. Komarov, V. G. Seleznev, G. A. Skorabogatov, "Method for Determining the Absolute Characteristics of CF_3I Laser Emission," Soviet Physics Technical Physics, 19, 558 (1974)

18. K. Hohla, and others, "60-J 1-nsec Iodine Laser," Journal of Applied Physics, 46, 2, 808 (Feb 1975)

19. A. V. Anatov, N. G. Basov, and others, "Amplifier with a Stored Energy over 700 J Designed for a Short-Pulse Iodine Laser," Soviet Journal Quantum Electronics, 5, 1, 123,(July 1975)

20. W. T. Silfvast, O. R. Wood, "Comparison of Radiation from Laser Produced and DC-Heated Plasmas in Xenon," Applied Physics Letters, 25, 5, 274, (1 Sep 1974)

21. Handbook of Military Infrared Technology, p. 252, Naval Research Laboratory, 1965 (W. Wolfe, Ed.)

22. F. T. Aldridge, "High-Pressure Iodine Photodissociation Laser," Applied Physics Letters, 22, 4, 180, 15 Feb 1973

23. G. Brederlow, K. Hohla, K. J. Witte, "Pulsed High Power Iodine Laser at IPP," Paper presented at the 7th European Conference on Plasma Production by High Power Lasers, Garching, F.R.G., 22-26 April 1974

24. T. D. Padrick, R. E. Palmer, "Pressure Broadening of the Atomic Iodine $5^2P_{1/2}$ - $5^2P_{3/2}$ Transition," Journal of Chemical Physics, 62, 8, 3350, 15 April 1975

25. W. Fuss and others, "Parametric Studies of a 60 J - 1 ns Iodine Laser," Paper presented at the 7th International Quantum Electronics Conference at San Francisco, CA, June 1974.

26. K. Hohla, K. L. Kompa, "Energy Transfer in a Photochemical Laser," Chemical Physics Letters, 14, 4, 445, 15 June 1972.

27. N. G. Basov, and others, "High-Power Discharges in Gases I, Experimental Investigation of Optical and Energy Characteristics of a High-Power Discharge in Air," Soviet Physics - Technical Physics, 15, 3, 399, September 1970

28. N. G. Basov and others, "Light Emission from Exploding Wires," Soviet Physics - Technical Physics, 13, 12, 1665, June 1969.

29. N. G. Basov and others, "Strong Gas Discharges. II. A Description of the Dynamics of a Strong Discharge in a Gas by Means of a Self-Similar Solution of the Gas Dynamics Equations with Non Linear Thermal Conductivity," Soviet Physics - Technical Physics, 15, 4, 624, October 1970

30. D. M. Budzik, Construction of a Theta-Pinch for the Generation of Shock Waves in a Nitrogen Plasma, M.S. Thesis, Naval Postgraduate School (1970)

31. Bloom, A. L., Gas Lasers, p 69-100, Wiley, 1968

32. Air Force Aerospace Research Laboratories Report 75-0009, Design, Construction and Operation of an Experimental System for Study of Laser Energy Enhancement by Magnetic Fields, by Daniel R. Nordlund, p 12-14, 23

33. Yariv, A., Introduction to Optical Electronics, p 58-70, Holt, Rinehart and Winston, 1971

INITIAL DISTRIBUTION LIST

		No. Copies
1.	Defense Documentation Center Cameron Station Alexandria, VA 22314	2
2.	Library, Code 0212 Naval Postgraduate School Monterey, California 93940	2
3.	Chairman, Department of Physics & Chemistry Code 61 Naval Postgraduate School Monterey, California 93940	2
4.	Dr. F. Schwirzke, Code 61 Sw Department of Physics and Chemistry Naval Postgraduate School Monterey, California 93940	2
5.	Dr. A. W. Cooper, Code 61 Cr Department of Physics and Chemistry Naval Postgraduate School Monterey, California 93940	2
6.	Lt. F. C. Marcell, Jr. USN 139 N. 8th Avenue Mt. Vernon, New York 10550	2

Thesis 166526
M3363 Marcell
c.1 Design and construction of an iodine laser oscillator.